values for electron transfer between valence isomers are: 1'-CO_2CH_3, $\Delta E = -0.185$ V, $\Delta G = 4.27$ kcal/mol; 2-CO_2CH_3, $\Delta E = -0.200$ V, $\Delta G = 4.61$ kcal/mol; 1'-$COCH_3$, $\Delta E = -0.165$ V, $\Delta G = 3.81$ kcal/mol; 2-$COCH_3$, $\Delta E = -0.215$ V, $\Delta G = 4.96$ kcal/mol.

(19) Calculated by $\Delta_{1/2} = [2310(\bar{\nu}_{max} - \bar{\nu}_o)]^{1/2}$ where $\bar{\nu}_o$ is estimated from electrochemical data.
(20) B. Mayoh and P. Day, *Inorg. Chem.*, **13**, 2273 (1974).
(21) K. Schlogl and M. Walser, *Montsh. Chem.*, **100**, 1515 (1969).
(22) M. D. Rausch, *J. Org. Chem.*, **6**, 1802 (1961).
(23) V. D. Parker, unpublished results.

The Spectrochemical Properties of Tetragonal Complexes of High Spin Nickel(II) Containing Macrocyclic Ligands

Ludmila Y. Martin, C. Robert Sperati, and Daryle H. Busch*

Contribution from The Evans Chemical Laboratory, The Ohio State University, Columbus, Ohio 43210. *Received September 27, 1976*

Abstract: A selected broad series of complexes with tetraaza macrocyclic ligands has been synthesized, characterized, and subjected to detailed electronic spectral studies. All complexes contain high spin, tetragonal nickel(II) and are of the general formula $Ni(MAC)X_2$, where X = Br, Cl, N_3, and NCS when possible. For macrocyclic ligands of greatest ligand field strengths only the NCS complexes are high spin. The saturated, unsubstituted tetraaza macrocycles [13]aneN$_4$, [15]aneN$_4$, and [16]aneN$_4$ and their Ni^{2+} complexes were first synthesized during these studies. Combined with [14]aneN$_4$, they comprise a unique series of ligands that is ideally suited for the study of ring-size effects among complexes with macrocyclic ligands. The smallest ring [13]aneN$_4$ gives no high spin complexes of the desired trans geometry—the other ligands do provide such species. A variety of additional, previously reported ligands was incorporated into these studies in order to cover a broad range of structural parameters. The effects due to varying extent and positions of unsaturation and those due to the presence of sterically demanding substituents have been considered. Electronic spectra were measured both in solution and in the solid state at room temperature and in the solid state at 77 K. The low temperature data were used in all calculations. Experimental curves were resolved into well-positioned absorption bands by Gaussian analysis. These input data were used in both weak and strong ligand field models, with complete configuration interaction, in order to calculate spectrochemical parameters. Observation of five or six bands permitted a tested best-fit calculation, while four bands allow analytical solution for the parameters in a closed calculation. The majority of the data was sufficient to facilitate extremely precise fitting to the model. Approximate techniques were developed for obtaining useful estimates of the maximum number of parameters from as few as two or three observed bands. A single crystal polarized spectrum eliminated ^3E_g as a possible ground state for Ni([14]aneN$_4$)Cl$_2$. The precisely determined spectrochemical parameters reveal or confirm a number of significant relationships. The ligand field strength of the macrocycle, Dq^{xy}, varies systematically with ring size—[15]aneN$_4$ fits Ni^{2+} well yielding a normal Dq^{xy} value; [14]aneN$_4$ is constrictive toward Ni^{2+} and produces an unusually large value for Dq^{xy}; [16]aneN$_4$ is dilative toward Ni^{2+} and exerts a weak ligand field. Replacement of saturated amine linkages by imine groups increases Dq^{xy} but conjugation is unimportant as is the presence of axial CH_3 groups as substituents. The various structural contributions to Dq^{xy} can be quantitated and used in predictions. Dq^z reflects the normal spectrochemical series for axial ligands but the values depend on Dq^{xy} in a reciprocal fashion. Additional parameters are discussed.

Complexes of macrocyclic ligands having structure I are ideally suited to the study of the effects of tetragonal ligand fields on the electronic states of metal ions. Structure I is easily

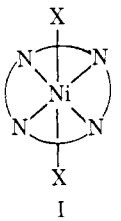

I

obtained for many tetraaza macrocyclic ligands and the ligand structures available either as a result of earlier studies or as part of this work involve more highly systematic variations in structural parameters than are conveniently obtainable with noncyclic in-plane ligands. The macrocyclic ligands used are summarized in Figure 1, where their systematic abbreviations are given.[1] Ligands 1, 2, 8, and 9 provide the opportunity to study the effects of changing the ring size among the macrocyclic ligands; those numbered 5, 6, 7, 10, and 12 present different patterns and extents of unsaturation; while ligands 3 and 4 differ from 2 only in the extent of methyl substitution. Ligands 13 and 14 provide the additional complication of a pyridine ring fused to the inner macrocyclic ring. The thorough assignments and interpretation of the electronic spectra of these tetragonal complexes are made possible by a progression of studies on more limited examples of such Ni^{2+} complexes.

Data Reduction and Interpretation of Spectra

Most octahedral and pseudo-octahedral complexes of Ni^{II} yielded paramagnetism corresponding to two unpaired electrons and are green to violet in color. Their electronic spectra, that are traceable to the triplet term system, display three (in the case of octahedral) or more absorption bands with characteristically low extinction coefficients (ideally $\epsilon = 1\text{–}10$ L^{-1} mol^{-1} cm^{-1}). The theoretical energy level diagram[2] for a d^8 metal ion in O_h and D_{4h} symmetry is presented in Figure 2. The diagram indicates that as many as six triplet–triplet transitions may be observed in the electronic spectra of complexes with D_{4h} symmetry. Observed spectra for such compounds rarely display more than five absorptions bands.[3-5] This often results from splittings that are small compared to bandwidths or to the overlap of more intense charge-transfer or ligand spectral bands. The spectra are also often complicated further by the occurrence of spin-forbidden transitions that may exhibit misleading apparent intensities because of their

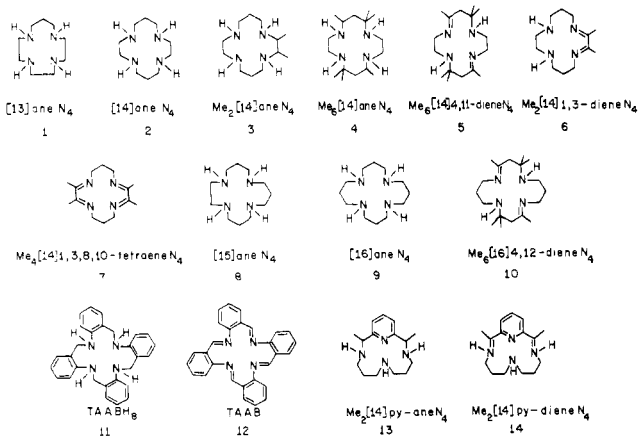

Figure 1. Macrocyclic ligands used in this study of Ni^{2+} complexes.

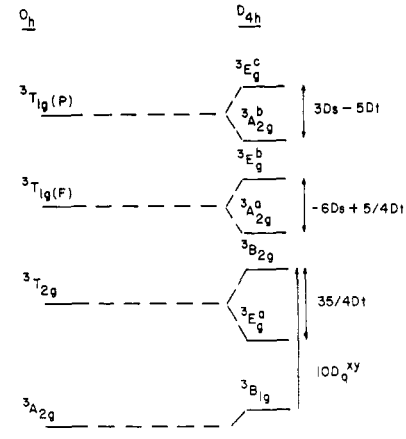

Figure 2. Energy level diagram for Ni^{2+} in O_h and D_{4h} symmetry—weak field model.

overlap with other bands or they may attain substantial relative intensities as a result of intensity stealing by interaction with stronger absorption bands. These complications require careful and detailed analysis of experimental spectra as an essential aspect of their assignment. Gaussian analyses were performed on all electronic spectra discussed herein using a nonlinear least-squares computer program.[6] Since it is well known that any curve may be considered to be the sum of an infinite number of Gaussian components, a reasonable indication of band presence was required for inclusion among the several Gaussian components in the data reduction. All band maxima reported here are derived from Gaussian analysis of the experimental curves.

Room temperature solid state and chloroform solution spectra were essentially identical. Spectral bands generally showed decreases in both intensity and bandwidth at liquid nitrogen temperature. The decreased bandwidths resulting from lower populations of vibronic states were accompanied by the expected shifts[7] in band maxima by 50–100 cm^{-1}.

The overall procedure associated with interpretation of the electronic spectra proceeded from curve analysis to closely define band maxima, through tentative assignment of the band maxima and calculation of theoretical parameters, to calculation of predicted band maxima and their comparison with the experimental values (from Gaussian analysis). The assignments and calculated positions of the maxima are based on two assumptions that are tenuous in the rigorous sense but pragmatically common practice: (1) the effective symmetry about the metal ion (microsymmetry) is D_{4h} and (2) the ligand field model is adequate for the deduction of empirical spectral parameters.

None of the complexes, when viewed in detail, conforms to D_{4h} symmetry, and lower point groups such as C_{2v} would constitute approximations in many cases. These reductions in symmetry theoretically provide additional d-orbital splittings and should, at best, result in band broadening. However, if the additional splitting (beyond D_{4h}) is small compared to the principal splittings that derive from the presence of four nitrogen donors in (approximately) a single equatorial plane and two different donor atoms on the axis perpendicular to that plane, then the assumption of D_{4h} site symmetry may be adequate to account for the observed spectral band locations. Spin–orbit coupling, which has not been included in the interpretations offered here, is in principle also a source of small splittings. The experimental spectra available do not provide sufficient resolution to require consideration of the smaller effects.

Wentworth and Piper[8] provided a first-order crystal field model for tetragonally distorted cobalt(III) complexes which has been extended to include tetragonal nickel(II) complexes.[9,10] Referring to Figure 2, the splitting of the $^3T_{2g}$ octahedral band upon descent in symmetry to D_{4h}, is dependent solely on the tetragonal splitting parameter, Dt. Dt is proportional to the difference between the strengths of the in-plane ligand field (Dq^{xy}) and the axial ligand field (Dq^z). Splittings are observed when the transitions $^3B_{1g} \rightarrow {}^3E_g{}^a$ and $^3B_{1g} \rightarrow {}^3B_{2g}$ differ by some 1500 cm^{-1} or more. The difference between these two transition energies is $35/4\ Dt$. Positive values of Dt indicate that Dq^{xy} is greater than Dq^z and that the $^3E_g{}^a$ state lies lowest in energy relative to the $^3B_{1g}$ ground state. The splittings in the $^3T_{1g}(F)$ and $^3T_{1g}(P)$ states are smaller than that for $^3T_{2g}$. The splitting in these manifolds is a function of two parameters, Ds and Dt. The working relationships in the simple Wentworth–Piper treatment are

$$\nu_{B_{2g}} - \nu_{B_{1g}} = 10Dq^{xy} \quad (1)$$

$$\nu_{E_g{}^a} - \nu_{B_{1g}} = 10Dq^{xy} - 35/4Dt \quad (2)$$

$$Dt = (4/7)(Dq^{xy} - Dq^z) \quad (3)$$

$$Dq^z = (1/10)(2\nu_{E_g{}^a} - \nu_{B_{2g}}) \quad (4)$$

This treatment uses only two spectral bands $\nu_{E_g{}^a}$ and $\nu_{B_{2g}}$ to derive the spectrochemical parameters.

The tetragonal case has been treated in more detail by a number of authors. Drago and Rowley[3] have used the weak field approach while Lever[4,11] has applied the strong field treatment and Fenske, Martin, and Reudenberg[12] have developed the complete theory including spin–orbit coupling. The latter was directed principally at low spin, square planar systems. The need for the use of a more complete theoretical model than the Wentworth–Piper approach has been emphasized in these earlier studies. The application of such models requires the use of the entire triplet–triplet spectrum and such treatments are accessible when experimental spectra exhibit five or six bands of this kind. The electronic spectra of many of the complexes discussed here do exhibit the requisite numbers of absorption bands and the more rigorous models have been applied. To ensure against errors, both the strong field[5,11] and the weak field[2,3] models were used and the results obtained were identical, as is necessary since they are mathematically equivalent when full configuration interaction is included.

The orbital energy separations for the strong field model are given in Figure 3 and the term energies are

$$^3B_{1g} = 0$$
$$^3E_g{}^a = \Delta_1 + \Delta_2 - \Delta_3 + 3B$$
$$^3B_{2g} = \Delta_2$$
$$^3A_{2g}{}^a = \Delta_2 - \Delta_3 + 12B$$
$$^3E_g{}^b = \Delta_1 + \Delta_2 + 9B$$
$$^3A_{2g}{}^b = 2\Delta_1 + 2\Delta_2 - \Delta_3 + 3B$$
$$^3E_g{}^c = \Delta_1 + 2\Delta_2 - \Delta_3 + 3B$$

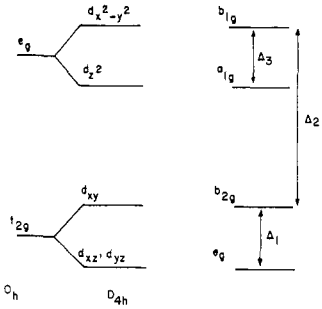

Figure 3. Orbital splitting diagram for Ni^{2+} in O_h and D_{4h} symmetry—strong field model.

The ligand field parameters employed in the two approaches are related in the following manner.[11]

$$\Delta_1 = 3Ds - 5Dt$$
$$\Delta_2 = 10Dq^{xy}$$
$$\Delta_3 = 4Ds + 5Dt$$
$$Ds = (1/7)(\Delta_1 + \Delta_3)$$
$$Dt = -(1/35)(4\Delta_1 - 3\Delta_3)$$

Calculation of Crystal Field Parameters. The computer programs employed in these calculations are recorded elsewhere.[6] From the input energies (observed spectral band energies), the program, through an iterative process that involves varying the parameters Δ_1, Δ_2, Δ_3, and B (strong field) or Ds, Dq^{xy}, Dt, and B (weak field), generates the spectrochemical parameters which best fit the observed energies. This "goodness" of fit between the observed and calculated band energies is determined by nonlinear least-squares criteria, with the criterion for agreement being a difference of ± 50 cm^{-1} or less between the observed and the calculated transition energies. For purposes of comparison, the same program generates spectral band energies and spectrochemical parameters where configuration interaction is both included (off diagonal matrix elements are included) and excluded (off diagonal matrix elements are set to zero).

Approximate Calculational Techniques. In attempts to obtain meaningful spectrochemical parameters in cases where insufficient data were available (three or fewer observed spectral bands) two programs denoted as "DT correction" and "Program Energy Search" were written.[6] The DT correction program is most approximate and requires only two transitions ($\nu_{E_g{}^a}$ and $\nu_{B_{2g}}$) in order to estimate reasonable values of Dq^z and Dt. In most cases the variation from CI values found in Dq^z from this program is less than 3%. However, for several of the more severely distorted bromide complexes, the error approaches 8%. This is still far better than the errors observed using the simple Dt formula of Wentworth and Piper which can be of the order of 100% (vide infra). The Dt correction can be represented to within 0.5% by a fourth degree polynomial (eq 5), Dt_{corr} is the corrected Dt and Dt_{ap} is the apparent Dt calculated employing eq 6.

$$Dt_{corr} = 0.989(Dt_{ap}) - (3.80 \times 10^{-4})(Dt_{ap})^2 + (3.53 \times 10^{-7})(Dt_{ap})^3 - (1.5 \times 10^{-10})(Dt_{ap})^4 \quad (5)$$

$$Dt = (4/35)(\nu_{B_{2g}} - \nu_{E_g{}^a}). \quad (6)$$

If three transitions are observed, $^3E_g{}^a$, $^3B_{2g}$, $^3E_g{}^b$, the computer program Energy Search can be used to calculate the entire set of spectrochemical parameters. This approximate approach derives four crystal field parameters using three pieces of data. The weak field mathematical model is used in slightly modified form. The four parameters Dq, Ds, Dt, and B are changed to Dq, B, Dt, and R, where R is the ratio Ds/Dt and these parameters are decreased from initial values by constant decrements in an iterative procedure. $10Dq$ remains invariant; R decreases from 3.0 to 1.0 by 0.1 decrement, and B decreases from 910 to 700 by decrements of 10 cm^{-1}. Initial values by Dt are calculated from $Dt = (4/35)(\nu_{E_g{}^a} - \nu_{B_{2g}})$ and, since these values are known to be high,[3,6] Dt is decreased over a 300-cm^{-1} range in 10-cm^{-1} decrements during iteration. Dt is iterated over its range for each value of B and B, over its range for every R.

"Best fit" parameters are obtained by comparison of calculated with experimental transition energies. Initial estimates of the parameters are made from the experimental energies, the interaction matrices are constructed and solved, and the absolute differences between calculated E_g eigenvalues and corresponding input experimental energies are summed to produce the convergence criterion. Error sums less than 70 cm^{-1} cause the corresponding parameter values to be stored and when ten iterations show no improvement the run terminates. Average parameters are calculated from parametric sets which yielded error sums within the specified limits and these are used to calculate the final predicted energies. The quantities showing the largest deviations from the results of full configuration interaction calculations are B and $E_g{}^c$ (1–10%); all other quantities were within 5% of the full CI values. Program Energy Search has the useful advantage that it provides a complete set of reasonable spectrochemical parameters while requiring only three pieces of data.

Results

Synthesis and Characterization of the Compounds. The complexes studied include the tetragonal complexes of formulas $Ni(MAC)X_2$ derived from 13 different macrocyclic ligands. For the saturated macrocyclic ligands [14]$aneN_4$, [15]$aneN_4$, [16]$aneN_4$, Me_2[14]$aneN_4$, and *meso*-Me_6[14]$aneN_4$, the axial ligands X may be Br, Cl, NCS, or N_3. For most of the remaining ligands only the NCS derivative was available for study, usually because weaker axial ligands failed to produce the triplet ground state. Studies on the Ni^{II} complexes of the small macrocycle [13]$aneN_4$, to be reported elsewhere, revealed that all high spin derivatives of this ligand are cis in structure. Consequently, it is inappropriate to discuss those compounds here. Most of the complexes with the ligands Me_6[14]4,11-dieneN$_4$,[13] Me_6[14]$aneN_4$,[14] [14]$aneN_4$,[15] Me_2[14]1,3-dieneN$_4$,[16] Me_4[14]1,3,8,10-tetraeneN$_4$,[17] TAAB,[18] Me_2[14]py-$aneN_4$,[19] and Me_2[14]py-dieneN$_4$[19] have previously been synthesized; however, fresh samples were prepared and identified by elemental analysis, infrared spectral, and magnetic moment measurements.[6] The complexes of the ligands Me_2[14]$aneN_4$, [15]$aneN_4$, and [16]$aneN_4$ were all first prepared in the course of these studies. In addition, Ni([14]$aneN_4$)$(N_3)_2$, Ni(Me_2[14]1,3-dieneN$_4$)$(NCS)_2$, and Ni(Me_4[14]1,3,8,10-tetraeneN$_4$)$(NCS)_2$ were synthesized during this work. Elemental analysis (Table I) of the new compounds confirms the fact that all are of the composition $Ni(MAC)X_2$. The magnetic moments (Table I) all fall in the range from 3.07 to 3.27 μ_B thereby establishing the triplet ground states for the compounds. Electrical conductivity measurements on all of the new compounds in nitromethane solutions yield molar conductance values of less than 6 ohm^{-1} cm^2 mol^{-1}. This clearly demonstrates the fact that both anions are coordinated and the complexes $Ni(MAC)X_2$ are nonelectrolytes. In a few cases (Ni(Me_2[14]$aneN_4$)X_2 (all X) and Ni([14]$aneN_4$)$(N_3)_2$) mass spectral measurements revealed parent ion peaks. From these data the molecular formulations appear well justified. Identification of the compounds as trans-diacido species rests on the consistent electronic spectral properties of the complexes as is detailed in the discussion to follow.

The unsubstituted ligands [15]$aneN_4$ and [16]$aneN_4$ are especially important new macrocycles for they complete the

Table I. Elemental Analyses and Magnetic Moments for the New Complexes of the Composition Ni(MAC)X_2

Complex	Elemental analyses C Calcd	C Found	H Calcd	H Found	N Calcd	N Found	μ_{eff} (μ_B)
Ni([14]aneN$_4$)(N$_3$)$_2$	35.00	35.10	6.99	7.08	16.33	16.24	3.12
Ni(Me$_2$[14]aneN$_4$)Br$_2$	32.25	32.28	6.30	6.15	12.53	12.42	3.09
Ni(Me$_2$[14]aneN$_4$)Cl$_2$	40.25	40.36	7.87	7.79	15.65	15.72	3.18
Ni(Me$_2$[14]aneN$_4$)(N$_3$)$_2$	38.83	38.65	7.59	7.64	37.74	37.93	3.15
Ni(Me$_2$[14]aneN$_4$)(NCS)$_2$	41.69	41.55	6.99	7.08	20.83	20.96	3.17
Ni(Me$_2$[14]1,3-dieneN$_4$)-(NCS)$_2$	42.11	42.02	6.01	6.09	21.05	20.98	3.07
Ni(Me$_4$[14]1,3,8,10-tetraene-N$_4$)(NCS)$_2$	44.97	45.08	6.55	6.59	19.67	19.72	3.08
Ni([15]aneN$_4$)Br$_2$	30.52	30.25	6.01	5.76	12.95	13.29	3.24
Ni([15]aneN$_4$)Cl$_2$	38.42	38.14	7.57	7.33	16.30	15.99	3.22
Ni([15]aneN$_4$)(N$_3$)$_2$	37.01	37.04	7.29	7.22	39.25	39.50	3.07
Ni([15]aneN$_4$)(NCS)$_2$	40.13	40.24	6.69	6.62	21.61	21.69	3.09
Ni([16]aneN$_4$)Br$_2$	32.25	32.50	6.27	6.57	12.54	12.63	3.27
Ni([16]aneN$_4$)Cl$_2$	40.27	40.09	7.83	7.90	15.66	15.37	3.21
Ni([16]aneN$_4$)(N$_3$)$_2$	38.85	39.19	7.55	7.75	37.77	37.97	3.12
Ni([16]aneN$_4$)(NCS)$_2$	41.72	41.80	6.95	7.23	20.86	20.55	3.24

Table II. Characterization of the Macrocyclic Ligands[14–16]aneN$_4$

Ligand	Formula weight	*m/e* parent ion	Mp, °C	% C Calcd	% C Found	% H Calcd	% H Found	% N Calcd	% N Found	NMR, δ, 100 Hz, $CDCl_3$, Me_4Si
[14]aneN$_4$	200	200	161 dec	59.96	59.84	12.08	12.09	27.96	27.87	1.74 (quintet, 4 H, $J \approx 6$ Hz), 2.36 (s, 4 H) 2.74 (complex multiplet, 16 H)
[15]aneN$_4$	214	214	98–99	61.68	61.65	12.15	12.18	26.17	25.94	1.71 (quintet, 6 H, $J \approx 6$ Hz), 1.94 (s, 4 H), 2.74 (complex multiplet, 16 H)
[16]aneN$_4$	228	228	82–83	63.16	63.11	12.28	12.23	24.56	24.10	1.70 (quintet, 8 H, $J \approx 6$ Hz), 1.82 (s, 4 H) 2.72 (triplet, 16 H, $J \approx 6$ Hz)

series of unsubstituted tetraazamacrocycles which now extends from the 12-membered ring through the 16-membered ring. The 12-membered and 14-membered rings have long been known,[20,21] and the synthesis of the 13-membered ring and its complexes is reported elsewhere. This series has great utility in the delineation of the effect of ring size on the physical and chemical properties of complexes with macrocyclic ligands. For this reason, attention is given here to the synthesis and characterization of 1,4,8,12-tetraazacyclopentadecane ([15]aneN$_4$) and 1,5,9,13-tetraazacyclohexadecane ([16]-aneN$_4$).

Ligand syntheses followed a modification of a procedure developed by Yoshino and Koyama for the synthesis of a series of related triaza macrocyclic ligands. The general outline is shown in Scheme I. Variations and details are presented in the experimental section. Data pertinent to the characterization of the free ligands are given in Table II for [14–16]aneN$_4$. The compositions and molecular weights of the substances are established by analyses and mass spectra, respectively. Infrared and NMR data are consistent with the proposed structures.

Scheme I

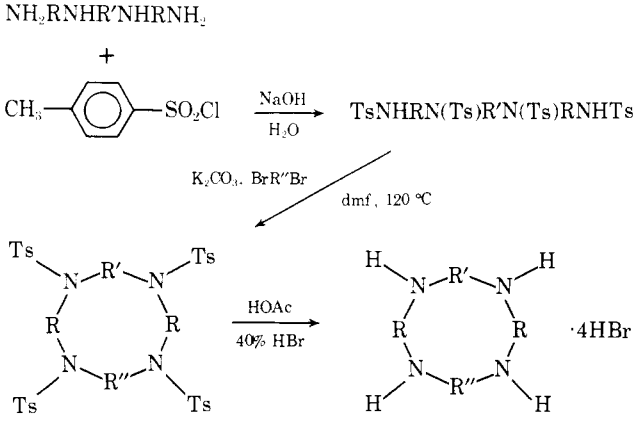

Assignments of Spectral Bands and Calculation of Parameters. The electronic spectra of this broad series of high spin Ni(II) complexes as measured on mulls at liquid nitrogen temperatures were used for detailed study because of the added spectral resolution of these data. Spectrochemical parameters were calculated, with full configuration interaction, after appropriate data reduction (see section on Data Reduction and Interpretation of Spectra). The resulting spectral assignments for these nickel(II) complexes appear in Table III, where the experimental values of the transition energies are also compared with those calculated from the derived spectrochemical parameters.

Interpretation of spectral data, based on a tetragonal model, necessitates the assignment of the $^3B_{1g} \rightarrow {}^3B_{2g}$ transition. This transition is related directly to $10Dq^{xy}$ (Dq^{xy} provides a measure of the in-plane field strength; i.e., the ligating capability of the macrocycle). Theory indicates that this transition should be insensitive to changes in axial donors and, for axial donors of ligand field strengths weaker than the in-plane ligand field, this transition should appear at higher energy than the $^3B_{1g} \rightarrow {}^3E_g{}^a$ transition (Figure 2). This suggests that the $^3B_{1g} \rightarrow {}^3B_{2g}$ transition should be most readily determined by considering several complexes with the same in-plane ligand but different axial donors and locating the band (in the proper energy range) which varies least with changes in axial donors. Lever has indicated that this may be helpful but that the $^3B_{1g} \rightarrow {}^3B_{2g}$ transition energy probably should not be totally independent of the axial ligand.[4]

Table III. Comparison of Experimentally Determined and Calculated Spectral Band Positions for the Ni(MAC)X_2 Complexes[a]

Complexes	ν (cm^{-1})					
	$^3B_{1g} \rightarrow {}^3E_g$[a]	$\rightarrow {}^3B_{2g}$	$\rightarrow {}^3A_{2g}$[a]	$\rightarrow {}^3E_g$[b]	$\rightarrow {}^3A_{2g}$[b]	$\rightarrow {}^3E_g$[c]
			Saturated Ligands			
Ni([14]aneN$_4$)Br$_2$	7 850	14 850[b]	13 700[b]	19 328	27 100 (sh)[b]	29 300
	7 808	14 872	13 748	19 399	27 137	29 275
Ni([14]aneN$_4$)Cl$_2$	8 600	14 750[b]	15 200[b]	19 400	27 250 (sh)[b]	29 152
	8 656	14 793	15 162	19 337	27 359	29 175
Ni([14]aneN$_4$)(N$_3$)$_2$	10 100	14 480[b]	16 300[b]	19 825	*c*	*c*
	10 034	14 441	16 352	19 899	28 820	29 959
Ni([14]aneN$_4$)(NCS)$_2$	11 080	14 150[b]	17 800 (sh)	20 225	*c*	*c*
	11 030	14 104	17 849	20 279	30 561	31 467
Ni(Me$_2$[14]aneN$_4$)Br$_2$	7 800	14 900[b]	13 650[b]	19 300	27 000 (sh)[b]	29 150
	7 761	14 875	13 696	19 347	26 991	29 126
Ni(Me$_2$[14]aneN$_4$)Cl$_2$	8 400	14 700[b]	14 900[b]	19 200	27 100 (sh)	29 000
	8 442	14 710	14 909	19 139	27 156	29 053
Ni(Me$_2$[14]aneN$_4$)(N$_3$)$_2$	10 100	14 300	16 577	19 570	*c*	*c*
	10 045	14 262	16 618	19 630	28 769	29 971
Ni(Me$_2$[14]aneN$_4$)(NCS)$_2$	11 200	14 125[b]	18 000 (sh)[b]	20 175[b]	*c*	30 900
	11 231	14 145	17 974	20 134	30 136	30 921
Ni(Me$_6$[14]aneN$_4$)Br$_2$	7 380	15 000[b]	12 931	19 000	26 200 (sh)	28 300
	7 312	14 922	12 976	19 099	26 136	28 276
Ni(Me$_6$[14]aneN$_4$)Cl$_2$	8 400	14 700[b]	15 100[b]	18 869	26 700 (sh)	28 700
	8 389	14 692	15 108	18 881	26 744	28 696
Ni(Me$_6$[14]aneN$_4$)(N$_3$)$_2$	9 400	14 132	15 600[b]	19 500	*c*	29 750
	9 399	14 131	15 601	19 501	28 373	29 750
Ni(Me$_6$[14]aneN$_4$)(NCS)$_2$	10 950	14 000	17 300 (sh)	19 995	29 800 (sh)	30 500
	10 933	13 989	17 314	20 016	29 741	30 489
Ni(Me$_2$[14]py-aneN$_4$)(NCS)$_2$	10 970	14 051	16 920[b]	19 962	29 500 (sh)	30 250
	10 863	13 979	16 972	20 008	29 156	30 180
Ni([15]aneN$_4$)Br$_2$	8 072	12 820[b]	13 889[b]	17 482[b]	25 500[b] (sh)	27 082
	8 085	12 830	13 882	17 468	25 528	27 086
Ni([15]aneN$_4$)Cl$_2$	8 664	12 390[b]	14 421[b]	17 602	26 100[b] (sh)	27 299
	8 707	12 425	14 395	17 556	26 116	27 313
Ni([15]aneN$_4$)(N$_3$)$_2$	9 698	12 272	15 486[b]	17 824	*c*	27 516
	9 701	12 274	15 484	17 821	26 804	27 515
Ni([15]aneN$_4$)(NCS)$_2$	10 326	12 029 (sh)[b]	15 834[b]	18 367	*c*	28 514
	10 312	12 019	15 842	18 383	28 096	28 508
Ni(TAABH$_8$)(NCS)$_2$	10 130	11 250	15 800	17 400	*c*	28 000
	10 076	11 159	15 872	17 439	27 533	27 956
Ni([16]aneN$_4$)Br$_2$	7 312	11 273	13 089	15 550	*c*	25 624
	7 325	11 283	13 082	15 539	24 013	25 627
Ni([16]aneN$_4$)Cl$_2$	7 782	11 157	13 455	15 758	*c*	25 621
	7 791	11 164	13 450	15 749	24 292	25 623
Ni([16]aneN$_4$)(N$_3$)$_2$	9 037[b]	10 871 (sh)[b]	14 714[b]	16 479	26 066	26 848
	9 037	10 871	14 715	16 479	26 066	26 843
Ni([16]aneN$_4$)(NCS)$_2$	9 606[b]	10 724[b]	15 385[b]	16 754	*c*	27 063
	9 634	10 742	15 370	16 725	26 603	27 072
			Unsaturated Ligands			
Ni(Me$_2$[14]1,3-dieneN$_4$)(NCS)$_2$	11 250	15 616	17 600[b]	21 385[b]	*c*	*c*
	11 196	15 537	17 699	21 465	30 988	31 900
Ni(Me$_6$[14]4,11-dieneN$_4$)(NCS)$_2$	11 230	15 750	18 200	21 058	*c*	*c*
	11 158	15 694	18 294	21 133	30 690	31 917
Ni(Me$_4$[14]1,3,8,10-tetraeneN$_4$)(NCS)$_2$	11 950	17 700	19 000	23 000[b]	*c*	*c*
	11 909	17 664	19 067	23 098	32 643	33 924
Ni(Me$_2$[14]py-dieneN$_4$)(NCS)$_2$	11 300	18 600[b]	18 800[b]	24 500	*c*	*c*
	11 456	18 663	18 655	24 416	33 819	35 380
Ni(TAAB)(N$_3$)$_2$	10 000	14 700[b]	17 000[b]	20 000	*c*	*c*
	10 050	14 734	16 964	19 941	29 132	30 525
Ni(TAAB)(NCS)$_2$	10 900	14 650	17 400[b]	20 800[b]	*c*	*c*
	10 913	14 658	17 391	20 785	30 581	31 507
Ni(Me$_6$[16]4,12-dieneN$_4$)(NCS)$_2$	10 329	12 229	16 496[b]	18 200	*c*	28 500 (sh)
	10 341	12 237	16 488	18 186	27 937	28 506

[a] The first row of transition energies for a given compound is the experimentally observed spectral transitions from halo-carbon grease mull spectra at 77 K, while the second row of transition energies is program generated using full-configuration interaction. [b] Predicted by Gaussian analysis. [c] Not observed.

Electronic Spectra of Ni([14]aneN$_4$)X$_2$. The electronic spectra of these complexes were reported earlier with measurements confined to the range from 300 to 1000 nm.[23] From these limited data, it was concluded that the complexes are essentially octahedral in nature with little tetragonal distortion. Our measurements[24] reveal additional absorption bands at wavelengths greater than 1000 nm which are best interpreted in terms of strong tetragonal distortion. The crystal structure

of Ni([14]aneN$_4$)Cl$_2$ establishes the trans-diacidotetramine structure and confirms the strong tetragonal distortion.[25] The Ni–Cl distance is 0.15 Å greater than otherwise expected.

The mull spectra as determined at 77 K for the group of Ni([14]aneN$_4$)X$_2$ complexes are reproduced in Figure 4 and the band positions are summarized in Table III. Through Gaussian analysis all six expected triplet–triplet bands can be located. As indicated earlier, for $Dq^z < Dq^{xy}$, the low energy triplet should arise from the transition to $^3E_g{}^a$. This band should shift to lower energies as Dq^z decreases. This expectation is fulfilled since ν_1 follows the normal spectrochemical sequence $Br^- < Cl < N_3 < NCS$. If the common sequence of states occurs, $^3B_{1g}$ is the ground state and the $^3B_{2g}$ state, which serves to measure $10Dq^{xy}$, is most probably the second lowest excited state—it is certain to be second or third lowest in energy. The transition $^3B_{1g} \rightarrow {}^3B_{2g}$ should be relatively insensitive to a change in axial ligand. The dominant high energy band should be associated with $^3B_{1g} \rightarrow {}^3E_g{}^c$. Further, this state should be the highest energy triplet in the system; therefore the assignment is easily made. So long as the large spectral band dominated by $^3E_g{}^c$ is strongly dissymmetric or exhibits a shoulder, the position of $^3B_{1g} \rightarrow {}^3A_{2g}{}^b$ can be determined. This has been possible for the bromide and chloride. The very strong band at slightly less than 20 000 cm^{-1} is readily ascribed to $^3B_{1g} \rightarrow {}^3E_g{}^b$ ($^3E_g{}^b$ from $^3T_{1g}$(F)). Again, when $^3A_{2g}{}^a$ appears as an obvious feature on the low energy side of the $^3B_{1g} \rightarrow {}^3E_g{}^b$ absorption, the transition to $^3A_{2g}{}^a$ is readily assigned. As Figure 4 shows this is the case for Ni([14]aneN$_4$)(NCS)$_2$. Given this very tidy situation, the transition of most interest (to $^3B_{2g}$) is most readily assigned. In the spectrum of the thiocyanate that transition ($^3B_{1g} \rightarrow {}^3B_{2g}$) is represented by the well-defined band at 14 150 cm^{-1}. In the spectrum of the azide complex, the transitions to $^3B_{2g}$ and $^3A_{2g}{}^a$ overlap strongly, and Gaussian analysis is used to separate them. The band at 14 480 cm^{-1} is attributed to $^3B_{2g}$ (very close to that for the thiocyanate) and the band at 16 532 to $^3A_{2g}{}^a$. The chloride spectrum shows one slightly asymmetric band at ~15 000 cm^{-1} and the bromide spectrum shows two components again, but with the distinction that one of the major features appears at lower energy (13 700 cm^{-1}). These features for the chloride and bromide are consistent with a relatively fixed position for the $^3B_{2g}$ band and a shift in the position of the $^3A_{2g}{}^a$ band, as expected, (see eq 6), toward lower energies as Dq^z decreases (NCS → N$_3$ → Cl → Br). Thus the band at 13 700 cm^{-1} for Ni([14]aneN$_4$)Br$_2$ is assigned to $^3B_{1g} \rightarrow {}^3A_{2g}$ while this transition occurs at 15 200 for Ni([14]aneN$_4$)Cl$_2$. The $^3B_{2g}$ bands are assigned at 14 750 and 14 850 cm^{-1} for the chloride and bromide, respectively. It is significant that a crossover in states has occurred but that the Dq^{xy} band has remained relatively fixed in position. This adds confidence to our assignments. Attempts to fit the data with alternate assignments have generally given less satisfactory results.

The spectrochemical parameters for the chloride and bromide complexes were calculated using a full six band best fit. No evidence for splitting was found for the $^3T_{1g}$(P) state for the thiocyanate complex and this band was obscured by more intense bands for the azide complex. A five-band fit was used for the thiocyanate complex with the assumption that the $^3T_{1g}$(P) band corresponds to the position of the $^3B_{1g} \rightarrow {}^3E_g{}^c$ transition. For Ni([14]aneN$_4$)(N$_3$)$_2$ the fifth band ($^3E_g{}^c$) was estimated using Program Energy Search. Then a five-band best fit was calculated using this fifth band. Iteration was carried out over a 3000-cm^{-1} range in units of 100 cm^{-1} until a constant set of parameters and best fit (within 80 cm^{-1}) reproduction of experimental energies was obtained. The calculated band positions are included, for comparison, with the experimental values in Table III. The best fit spectrochemical parameters are summarized in Table IV. These will be discussed later. The excellent agreement between the calculated and

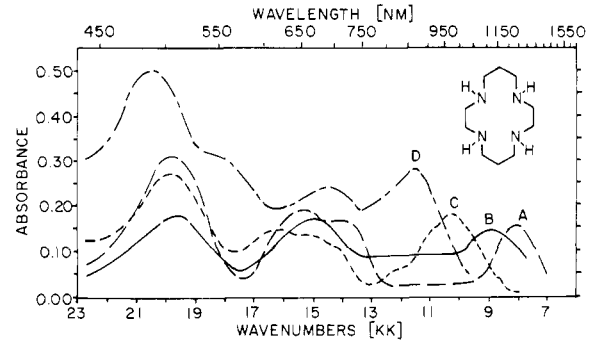

Figure 4. Electronic spectra of Ni^{2+} complexes with [14]aneN$_4$ at 77 K: A, Ni([14]aneN$_4$)Br$_2$; B, Ni([14]aneN$_4$)Cl$_2$; C, Ni([14]aneN$_4$)(N$_3$)$_2$; D, Ni([14]aneN$_4$)(NCS)$_2$. 1 μm^{-1} = 10 kK.

experimental band positions (Table III) strongly supports the validity of the entire treatment. Excessive significant figures are carried in Table III to facilitate visual comparison of the fit of the model to the data. The percent deviation between calculated and observed for the 20 pieces of data associated with these four compounds is 0.33%.

Polarized Single-Crystal Spectrum of Ni([14]aneN$_4$)Cl$_2$. In the course of early studies, the extremely large Dq^{xy} values for the macrocyclic ligands in *trans*-Ni(MAC)X$_2$, their associated low Dq^z values, and poor fits between observed and calculated values (configuration interaction had been ignored) prompted Lever[4] to suggest that the observed behavior for macrocycles is abnormal. He suggested the possibility that the ground state had changed from $^3B_{1g}$ to ^3E_g. It is well known that the ground state changes from the high spin $^3B_{1g}$ to low spin $^1A_{1g}$ (^{1}D) when the axial ligands are removed (or become extremely weak). If the $^3E_g{}^a$ state decreases in energy (with a certain structural change) faster than the $^1A_{1g}$ state, the ^3E_g state might crossover $^3B_{2g}$ and become the ground state (still a triplet). This requires the d-orbital ordering $d_{x^2-y^2} > d_{xz}, d_{yz} > d_{z^2} > d_{xy}$. It has long been accepted[12] that a more likely ordering is $d_{x^2-y^2} > d_{xy} > d_{z^2} > d_{xz}, d_{yz}$. More recently, Donini, Hollebone and Lever[26] have reported a detailed theoretical treatment of this question and concluded that $^3B_{1g}$ is likely to remain the ground state for the triplet term system of d^8 in D_{4h} symmetry unless axial ligands are absent or these ligands exert a ligand field that is positive in charge. The presence of strong π donors in a planar complex might generate a ^3E_g ground state.

While the extremely good fit between theory and experiment strongly supports the assignments made, the opportunity for a more detailed study of the optical spectrum of Ni([14]-aneN$_4$)Cl$_2$ was provided by the x-ray structure determination[25] on this compound.[27] On the basis of the vibronic intensity mechanism and employing the usual symmetry arguments,[28] the polarizations given in Table V are predicted. Thus, for a $^3B_{1g}$ ground state, the transitions to $^3A_{2g}$ and $^3B_{2g}$ are polarized such that they are forbidden in the z direction and allowed in the xy plane. The transition $^3B_{1g} \rightarrow {}^3E_g$ is allowed in the two polarizations. In contrast, theory predicts that all transitions, from a ^3E_g ground state to $^3B_{2g}$, $^3A_{2g}$, and ^3E_g alike, are allowed in both polarization modes. Therefore an absolute distinction between these two alternate ground states can be made by studying the polarized single-crystal spectra of these materials.

A single crystal of Ni([14]andN$_4$)Cl$_2$ (0.5 × 2.0 mm) was mounted on a microscope slide such that the plane of the four nitrogens was perpendicular to the plane of the slide. With the slide transverse to the optical path of the spectrophotometer, simple rotation of a polarizer could orient the electric vector of the radiation collinear with either the z axis of the complex or with its xy plane. Polarizing films HR (800–2200 nm) and

Table IV. Spectrochemical Parameters for Ni(MAC)X_2 Complexes[a] (in cm^{-1})

Complex	Dq^{xy}	Dq^z	Dt	Ds	Δ_1	Δ_3	B
Ni([14]aneN$_4$)Br$_2$	1487	287	685	1384	725	8966	849
Ni(Me$_2$[14]aneN$_4$)Br$_2$	1487	278	690	1375	672	8957	842
Ni(Me$_6$[14]aneN$_4$)Br$_2$	1492	207	734	1440	657	9431	793
Ni([15]aneN$_4$)Br$_2$	1283	452	475	925	399	6075	818
Ni([16]aneN$_4$)Br$_2$	1128	418	406	715	114	4899	853
Ni([14]aneN$_4$)Cl$_2$	1480	379	629	981	−202	7069	831
Ni(Me$_2$[14]aneN$_4$)Cl$_2$	1471	369	629	1019	−87	7226	837
Ni(Me$_6$[14]aneN$_4$)Cl$_2$	1469	344	624	877	−578	6723	825
Ni([15]aneN$_4$)Cl$_2$	1242	589	373	835	639	5206	825
Ni([16]aneN$_4$)Cl$_2$	1116	510	347	663	258	4387	834
Ni(TAAB)(N$_3$)$_2$	1473	624	485	705	−313	5245	867
Ni([14]aneN$_4$)(N$_3$)$_2$	1445	661	448	833	261	5572	829
Ni(Me$_2$[14]aneN$_4$)(N$_3$)$_2$	1426	666	434	724	2	5069	849
Ni(Me$_6$[14]aneN$_4$)(N$_3$)$_2$	1413	584	473	970	544	6248	865
Ni([15]aneN$_4$)(N$_3$)$_2$	1227	764	265	600	477	3731	797
Ni([16]aneN$_4$)(N$_3$)$_2$	1087	757	188	552	714	3151	869
Ni(Me$_2$[14]py-dieneN$_4$)(NCS)$_2$	1866	611	717	1216	64	8452	884
Ni(Me$_4$[14]1,3,8,10-tetraeneN$_4$)(NCS)$_2$	1767	735	589	832	−453	6277	809
Ni(Me$_6$[14]4,11-dieneN$_4$)(NCS)$_2$	1569	740	474	633	−469	4899	842
Ni(Me$_2$[14]1,3-dieneN$_4$)(NCS)$_2$	1553	784	439	848	347	5592	837
Ni(TAAB)(NCS)$_2$	1465	801	379	823	573	5192	882
Ni([14]aneN$_4$)(NCS)$_2$	1418	876	310	620	262	4084	860
Ni(Me$_2$[14]aneN$_4$)(NCS)$_2$	1414	878	306	522	32	3620	856
Ni(Me$_6$[14]aneN$_4$)(NCS)$_2$	1399	848	314	656	389	4198	846
Ni(Me$_2$[14]py-aneN$_4$)(NCS)$_2$	1398	843	316	722	584	4474	822
Ni(Me$_6$[16]4,12-dieneN$_4$)(NCS)$_2$	1223	874	199	455	371	2820	840
Ni([15]aneN$_4$)(NCS)$_2$	1202	908	168	695	1245	3618	842
Ni(TAABH$_8$)(NCS)$_2$	1115	923	110	486	906	2493	873
Ni([16]aneN$_4$)(NCS)$_2$	1074	873	115	430	716	2295	860

[a] Full configuration interaction included.

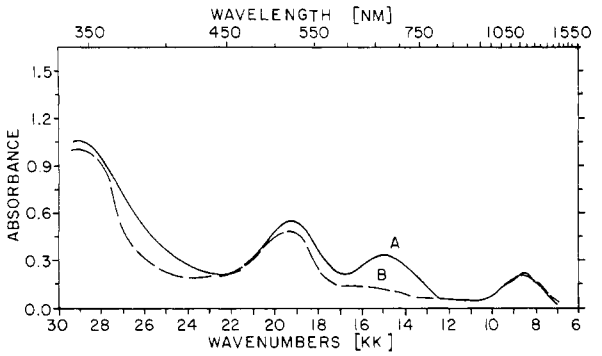

Figure 5. Polarized spectrum of Ni([14]aneN$_4$)Cl$_2$: A, $\perp$ to z axis; B, $\parallel$ to z axis. 1 μm^{-1} = 10 kK.

HN-7 (300–900 nm) obtained from Polaroid Corporation were used in conjunction with a Cary 14R-I spectrophotometer. The results are presented in Figure 5. The broad band at 1.5 μm^{-1} (attributed to $^3B_{1g} \rightarrow {}^3B_{2g}, {}^3A_{2g}$) is strongly polarized, showing the predicted preference for light polarized in the xy plane. The low energy side of the highest energy band (2.9 μm^{-1}) also shows an intensity decrease for light polarized along the z axis. This shoulder was assigned to $^3A_{2g}$[b]. We conclude that the polarization behavior is totally consistent with the assignments of Table II and that a ^3E_g ground state is absolutely eliminated for Ni([14]aneN$_4$)Cl$_2$. To further support the conclusions of Donini, Hollebone, and Lever,[26] we calculate that for ligands as strong as [14]aneN$_4$ ($Dq^{xy} \approx 1450$ cm^{-1}), the tetragonal splitting parameter Dt would have to be quite large (>1000 cm^{-1}) in order to produce a ^3E_g ground state. Further, this predicts a negative value for Dq^z which requires the absence of axial ligands and a square planar structure.

Table V. Polarization of Transitions of *trans*-Ni(MAC)X_2

Transition	Polarization[a] z	Polarization[a] x,y
$B_{1g} \rightarrow A_{2g}$	f	a
$B_{1g} \rightarrow B_{2g}$	f	a
$B_{1b} \rightarrow E_g$	a	a
$E_g \rightarrow A_{2g}$	a	a
$E_g \rightarrow B_{1g}$	a	a
$E_g \rightarrow B_{2g}$	a	a
$E_g \rightarrow E_g$	a	a

[a] Abbreviations: f, forbidden; a, allowed.

Electronic Spectra of Ni(Me$_2$[14]aneN$_4$)X_2 and Ni(Me$_6$[14]aneN$_4$)X_2. The ligands in these complexes differ from [14]aneN$_4$ only in the extent of methyl substitution on the chelate rings. The spectra of all the derivatives of Me$_2$[14]aneN$_4$ are virtually superimposable on those of [14]aneN$_4$ and the assignments are therefore now obvious. The spectra of the Me$_6$[14]aneN$_4$ complexes, while exhibiting small but significant quantitative differences from those of the unsubstituted ligand derivatives, are sufficiently similar so that assignments are quite straightforward. For both sets of complexes, six band fits to spectrochemical parameters were used for the bromide and chloride derivatives and five band fits were used for the azide and thiocyanate. In all cases, the agreement between the observed and calculated transition energies (Table III) was excellent.

Electronic Spectra of Ni([15]aneN$_4$)X_2. Three to five well-defined bands, several shoulders, and/or small sharp (spin forbidden) peaks are observed in the electronic spectra of Ni([15]aneN$_4$)X_2 (Figure 6). From its placement and shift

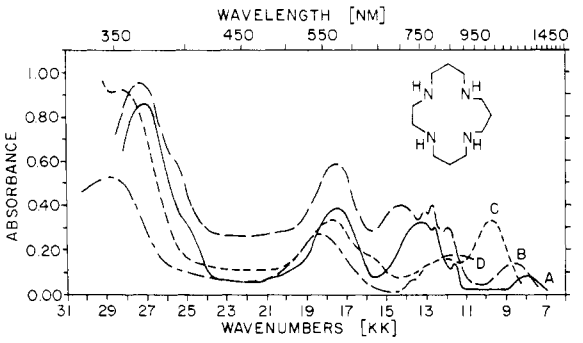

Figure 6. Electronic spectra of Ni^{2+} complexes with [15]aneN$_4$ at 77 K: A, Ni([15]aneN$_4$)Br$_2$; B, Ni([15]aneN$_4$)Cl$_2$; C, Ni([15]aneN$_4$)(N$_3$)$_2$; D, Ni([15]aneN$_4$)(NCS)$_2$. 1 μm^{-1} = 10 kK.

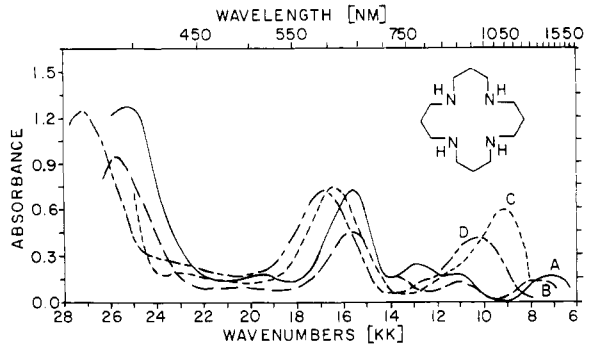

Figure 7. Electronic spectra of Ni^{2+} complexes with [16]aneN$_4$ at 77 K: A, Ni([16]aneN$_4$)Br$_2$; B, Ni([16]aneN$_4$)Cl$_2$; C, Ni([16]aneN$_4$)(N$_3$)$_2$; D, Ni([16]aneN$_4$)(NCS)$_2$. 1 μm^{-1} = 10 kK.

with X, the low energy band corresponds to the transition $^3B_{1g} \rightarrow {}^3E_g{}^a$. The succeeding three triplet-triplet transitions should arise from the excited states $^3B_{2g}$, $^3A_{2g}$, and $^3E_g{}^b$ and probably in that order. The spectrum of the azide complex displays a second band at 1.25 μm^{-1} fused onto the low energy band and a second band at 1.80 μm^{-1} having a distinct shoulder at 1.55 μm^{-1} (Gaussian analysis). This corresponds to the straightforward situation in which the two low energy octahedral triplet bands ($^3T_{2g}$ and $^3T_{1g}(F)$) show distinct splittings, but the splitting is small enough so that the parentage is clear. Thus the shoulder on the low energy band is assigned to $^3B_{1g} \rightarrow {}^3B_{2g}$; the strong band at 1.78 μm^{-1}, to $^3B_{1g} \rightarrow {}^3E_g{}^b$; and the shoulder at about 1.55 μm^{-1}, to $^3B_{1g} \rightarrow {}^3A_{2g}{}^a$. The high energy absorptions expected to arise from the $^3T_{1g}(P)$ state (O_h parent symmetry) were obscured in the spectrum of the azide complex. The interpretation of the Ni([15]aneN$_4$)(NCS)$_2$ spectrum follows the pattern described above for the azide.

Relatively strong tetragonal splitting again occurs for the bromide and chloride complexes (Figure 6, Table III). The low energy bands stand alone and are easily assigned ($^3B_{1g} \rightarrow {}^3E_g{}^a$). Also, the transition $^3B_{1g} \rightarrow {}^3E_g{}^b$ is obvious as the third band at about 1.75 μm^{-1}. However, the transitions to $^3B_{2g}$ and $^3A_{2g}$ overlap strongly, and the region of their occurrence is further complicated by the coincidence of triplet-singlet absorptions (sharp peaks). Gaussian analysis permitted resolution of this melange and the results are again contained in Table III. The $^3T_{1g}(P)$ manifold was treated as in the case of the [14]aneN$_4$ complexes. The agreement between experimental and calculated transition energies is again excellent.

Electronic Spectra of Ni([16]aneN$_4$)X$_2$. The assignment of the Ni([16]aneN$_4$)X$_2$ spectra (Figure 7) proceeds along similar lines. A pronounced bathochromic shift of the corresponding spectral bands is observed to accompany the increase in ring size. Little difficulty was encountered in making spectral assignments for the chloride and bromide derivatives, due to the well-resolved spectral features. In fact, these spectra illustrate the expected splittings and shifts very well. However, in the azide and thiocyanate spectra, band resolution is significantly diminished because of the decrease in band splittings accompanying increased axial field strengths and the low in-plane field strength (as compared to [15]aneN$_4$). The asymmetric bands located at 0.9–1.0 and 1.6–1.7 μm^{-1} were resolved by Gaussian analysis and assigned as shown in Table III. Alternative assignments fail to agree so well with the experimentally observed spectral bands. There was no detectable splitting of the $^3T_{1g}(P)$ manifold in the spectra of the Ni([16]aneN$_4$)X$_2$ complexes. Consequently, the intense band at $\approx$2.5–2.6 μm^{-1} was assigned to the $^3E_g{}^c$ component. The spectrochemical parameters that precisely reproduce the calculated bands appear in Table IV.

Electronic Spectra of Complexes with Unsaturated Ligands. Certain problems that are not unique to this study arise among the Ni(II) complexes of unsaturated macrocyclic ligands. The first problem is that metal-to-ligand and ligand-to-metal charge transfer transitions tend to obscure large portions of the spectra as the number of imine functions increases necessitating a heavy reliance on interpretations based on fewer bands and on Gaussian analysis in spectral band assignments. A second problem is that the increased unsaturation stabilizes the low-spin four coordinate structure for most axial ligands. Consequently, relatively strong axial ligands, such as NCS^-, are required to produce the high spin tetragonally distorted structures. This limits the number of accessible high spin derivatives. The most readily assignable spectrum among these compounds was that of Ni(Me$_6$[14]4,11-dieneN$_4$)(NCS)$_2$ (Figure 8). Utilizing the spectral assignments made on the saturated macrocycles as guidelines, and keeping in mind that imines often act as stronger donors toward metal ions than do secondary amines (resulting in an overall shift of the spectral bands to higher energy), the first four well-separated peaks, starting from the low energy side, were assigned to the $^3E_g{}^a$, $^3B_{2g}$, $^3A_{2g}{}^a$, and $^3E_g{}^b$ transitions. The shoulder appearing at 1.28 μm^{-1} might arise from a number of sources, e.g., lesser splitting due to the true lower symmetry, spin-orbit coupling, or a spin forbidden transition. Spectral bands at energies greater than 2.5 μm^{-1} are unreliable due to extreme slit widths of the spectrophotometer. Both four and five band iterative fits were performed, the fifth band was obtained by Program Energy Search. The experimentally determined and calculated energies are summarized in Table III and the spectrochemical parameters are collected in Table IV.

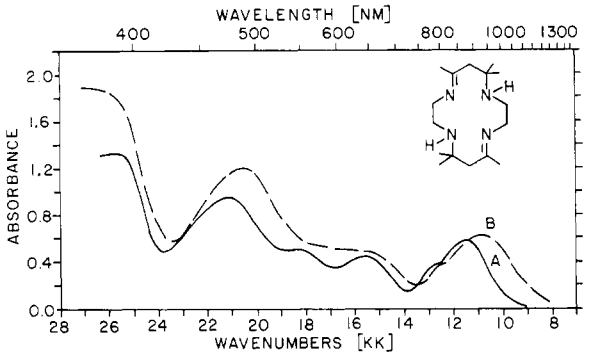

Figure 8. Electronic spectra of Ni(Me$_6$[14]4,11-dieneN$_4$)(NCS)$_2$: A, measured at 77 K; B, measured at room temperature. 1 μm^{-1} = 10 kK.

The spectrum of Ni(Me$_2$[14]py-dieneN$_4$)(NCS)$_2$ (Figure 9) provides an excellent example of the difficulties encountered in making spectral assignments as the number of imine functions increases. The low energy band is readily assigned to the $^3E_g{}^a$ transition. The high energy band is assigned to a charge transfer transition associated with the pyridine ring and the

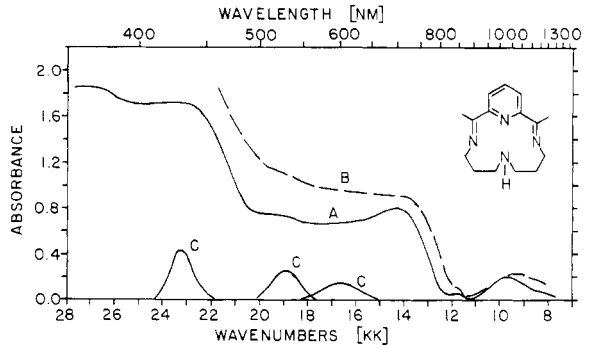

Figure 9. Electronic spectra of $Ni(Me_2[14]py\text{-}dieneN_4)(NCS)_2$: A, measured at 77 K; B, at room temperature; C, d-d bands identified by Gaussian analysis. 1 μm^{-1} = 10 kK.

conjugated imine groups. Such transitions are commonly observed for the iron complexes with unsaturated ligands and in fact dominate their spectra.[29] With a heavy reliance on Gaussian analysis and previous assignments for the analogous Co(III) complexes,[30,31] Gaussian components at 1.86, 1.88 and 2.45 μm^{-1} are assigned to the $^3B_{2g}$, $^3A_{2g}{}^a$, and $^3E_g{}^b$ transitions, respectively. Each band was fit employing an iterative procedure over a 2000-cm^{-1} range until a consistent set of parameters was obtained. Although the calculated spectrochemical parameters are intuitively agreeable and consistent with cobalt chemistry, they should be considered only as estimates, due to the limitations of the experimental spectrum.

Similar difficulties regarding spectral assignments were encountered for $Ni(Me_2[14]\text{-}1,3\text{-}dieneN_4)(NCS)_2$ and $Ni(Me_4[14]1,3,8,10\text{-}tetraeneN_4)(NCS)_2$. Again relying heavily on Gaussian analysis and previous assignments for the Co(III) analogues, the spectral assignments were made and tabulated. The remaining 14-membered ring is different from the other rings in that the only unsaturated group is a pyridine nitrogen. Even though the microsymmetry is much lower than D_{4h}, CRH exhibits a spectrum analogous to that observed for $Ni(Me_6[14]aneN_4)X_2$. The band assignments were made accordingly.

Proceeding now to the 16-membered ring macrocycles, TAAB and $Me_6[16]4,12\text{-}dieneN_4$, we would expect a hypsochromic shift of the spectral bands with respect to the saturated analogues due to the presence of imine functions. Furthermore, the shift to higher energy of the spectral transitions should be greater for TAAB than for $Me_6[16]4,12\text{-}dieneN_4$ since TAAB has twice as many imines. With this in mind the $^3B_{1g} \rightarrow {}^3B_{2g}$ transition in the thiocyanate and azide derivatives of TAAB is assigned to the 1.47 μm^{-1} band, while in the thiocyanate derivative of $Me_6[15]4,12\text{-}dieneN_4$ this transition occurs at 1.22 μm^{-1}. Gaussian analysis and iterative procedures were utilized, where necessary, in resolving and fitting the other spectral transitions. The very good agreement between the experimentally determined and calculated spectral transitions markedly improves the reliability of the spectrochemical parameters for these two ligand systems as compared to those for $Me_2[14]1,3\text{-}dieneN_4$, $Me_4([14]1,3,8,10\text{-}tetraeneN_4)$, and $Me_2[14]py\text{-}dieneN_4$.

The results presented in this section show that a dramatic increase in Dq^{xy} not only can be effected by a decrease in ring size but by the introduction of imine functions for a given ring size (Table IV; e.g., $Ni(Me_2[14]aneN_4)(NCS)_2$, Dq^{xy} = 1414 cm^{-1}; $Ni(Me_6[14]4,11\text{-}dieneN_4)(NCS)_2$, Dq^{xy} = 1569 cm^{-1}; and $Ni(Me_4[14]1,3,8,10\text{-}tetraeneN_4)(NCS)_2$, $Dq^{xy} \approx$ 1770 cm^{-1}).

We have used Dq^z as a criterion for the utility of approximate calculations by the fitting techniques used here on limited data sets. The results illustrated in Table VI show that the two approximate calculational methods, DT correction and Program Search (utilizing two and three observed transitions $^3E_g{}^a$, $^3B_{2g}$, and $^3E_g{}^b$, respectively) provide Dq^z values that agree within 1–3% of the CI values. These relatively simple approaches provide means of estimating the parameter Dq^z in cases where the CI calculations are obviated by the small number of d-d bands observed in some spectra.

Table VI. Comparison of Dq^z Values for $Ni(L)(NCS)_2$, Values Obtained from Various Methods of Calculation

Ligand	Dq^{xy} (cm^{-1})	CI[a]	Dq^z (cm^{-1}) Search[b]	Dq^z (cm^{-1}) DT corr[c]
$Me_6[14]4,11\text{-}diene\text{-}N_4$	1569	740	743 (0)	763 (3)
TAAB	1465	801	808 (1)	807 (1)
$[14]aneN_4$	1418	876	870 (−1)	889 (1)
$Me_2[14]aneN_4$	1414	878	870 (−1)	888 (1)
$Me_6[14]aneN_4$	1398	848	847 (0)	852 (0)

[a] Includes all configuration interaction (CI). [b] Results from Program Search. [c] Results obtained from eq 5.

Discussion

The array of compounds whose electronic spectra has been examined in this study provides a unique opportunity to evaluate the influence of a number of structural parameters on ligand fields strengths. It is particularly characteristic of the ligand field model that complexes of ligands having saturated first-row donors are most appropriately treated[32] and the majority of the complexes included herein are of that type. Within the formal D_{4h} stereochemistry, the nature of the in-plane ligand field, while always deriving from four nitrogen donors, is varied by alterations in the size of the macrocyclic ring and by changes in the extent and position of unsaturation. The principal manner of introducing unsaturation is by replacement of a secondary amine with an imine. This both provides a ligand π-electron system, with its attendant possibility of ligand–metal π-bonding, and changes the hybridization of the donor atoms so as to significantly increase the ligand s character in the ligand–metal σ bond. The relative significance of the π- vs. the σ-bonding effect can be judged by the importance of conjugative effects for conjugation lowers the energy of the ligand π^* orbitals, greatly favoring metal → ligand back-bonding.[29,33-35]

The most interesting parameter derived from the data reductions summarized above is Dq^{xy}, the in-plane ligand field splitting parameter. This quantity is taken as an indicator of the efficacy of the macrocycle as a ligand. As the strong field model of Figure 3 shows, $10Dq^{xy}$ corresponds to Δ_2 and represents the orbital splitting between the d_{xy} which is usually nonbonding (and occasionally π-antibonding) and the $d_{x^2-y^2}$ orbital, which is strongly σ-antibonding. Recognizing the relationships between energy level positions of nonbonding and related sets of bonding and antibonding orbitals, in the simplest of cases, Dq^{xy} varies directly with the extent of σ-bonding interaction. The second parameter Dq^z was defined by Wentworth and Piper to provide a corresponding characterization of the axial ligand field in tetragonal complexes.[8] Particular interest resides in this parameter because of earlier reports that Dq^z is strongly dependent on Dq^{xy}; thus the data reported here provide the opportunity to evaluate this *cis effect*[10,36] among nickel(II) complexes. Attention is given to additional parameters later in the discussion.

Variation of Dq^{xy} with Structure. The calculated values of Dq^{xy} appear in Table IV, where data are collected into groups

for compounds with constant axial ligands. Thus the variation of Dq^{xy} can be seen using series all having either bromide, chloride, azide, or thiocyanate as axial ligands. The latter series is most extensive for reasons mentioned earlier. Within each series, ligands are generally listed in order of decreasing Dq^{xy}, the exceptions occurring for very similar ligands in which cases they are listed in order of increasing ring substitution. It is immediately apparent that Dq^{xy} varies with the nature of the axial ligand and we will discuss this shortly. For the moment, it is useful to average Dq^{xy} over the several values obtained with different axial ligands and continue discussion on the basis of the averages.

We note that Dq^{xy} is strongly dependent on ring size, varying in the sequence (Dq^{xy}): [14]aneN$_4$, 1460 cm^{-1}; [15]aneN$_4$, 1240 cm^{-1}; [16]aneN$_4$, 1100 cm^{-1}. This has been discussed in a preliminary communication[37] and a totally analogous behavior has been observed for a more extensive series of ring sizes in the case of cobalt(III).[37,38] It has long been known that the *chelate effect* may have an enthalpy contribution[39] and this suggests that bonding may change for the same donor atoms depending on the geometric constraints of the ligand.[39] However, it may commonly be a tacit assumption that the ligating ability of a given donor is unchanged so long as electronic influences remain unaltered. This is witnessed in the writing of spectrochemical series that include, for example, saturated nitrogen donors. Under normal conditions, such an assumption is probably warranted but the data cited above dramatize the fact that geometric constraints, within a constant microsymmetry, can change Dq^{xy} over a range equal to 33% of its low value. The total range of Dq values for NiA$_6^{2+}$ does not exceed some 70% of the corresponding low value of Dq.[11] This indicates that the ring size effect is indeed large for it sends Dq^{xy} on an excursion that represents a major fraction of the range of the parameter. This effect has been traced to the strain energy in the planar chelated macrocyclic ligand in the case of cobalt(III)[38] and a similar argument may be advanced here. A model based on the classical strained molecule has been developed and used to relate ring sizes to experimental unstrained M–N distances.[37]

It is pertinent to again emphasize the fact that studies of Ni([13]aneN$_4$)X$_2$ complexes have shown that high spin species occur only with the ligand folded so that its four nitrogen atoms leave vacant two cis-octahedral positions.[40,41] This occurs because the metal ion site in planar tetradentate [13]aneN$_4$ is too small to accommodate high spin Ni^{2+}. The smaller low spin Ni^{2+} does fit into this site and the square planar diamagnetic species Ni([13]aneN$_4$)$^{2+}$ has been isolated and characterized.[40] The isolation of species in which [13]aneN$_4$ is coordinated in the planar manner in the corresponding cobalt(III) complexes is totally consistent with this view.

In order to judge further how strain energy affects the values of Dq^{xy} reported here for Ni([14–16]aneN$_4$)X$_2$ it is useful to attempt to identify a *normal* value, or range of values, for Dq^{xy} for coordinated organic amines in structures that are presumed to be unstrained. Sperati[6] has measured the electronic spectra of series of linear tetradentate and bidentate amines at 77 K, in complexes of the general form Ni(N$_4$)X$_2$, and subjected the spectral data to the same rigorous treatment described here. On the basis that the tetradentate ligands appear to show effects of the sort observed among macrocyclic derivatives, the bidentate ligands are preferred in identifying reference values. We therefore used a series of mono-N-substituted ethylenediamines to arrive at an ideal value for Dq^{xy} of organic amines in unstrained structures Ni(N$_4$)X$_2$. The average value of Dq^{xy} for N-R-en, where R = Me, Et, or *i*-Pr, is 1234 cm^{-1}. The value for en is about 1150 cm^{-1} and if this is included, an average value equal to 1213 cm^{-1} is obtained.[42]

Assuming that the normal value for four saturated nitrogen donors bound to Ni^{2+} is slightly greater than 1200 cm^{-1}, it follows that the ring that exhibits a Dq^{xy} closest to this value must coordinate in the least strained fashion. On this basis, it is concluded that [15]aneN$_4$ fits the Ni^{2+} ion best. The rings [14]aneN$_4$ and [16]aneN$_4$ chelate in relatively strained manners and partial accommodation of this enhanced strain in the N–Ni bond causes abnormal Dq^{xy} values. The smaller ring [14]aneN$_4$ must be expanded so that its inner metal site is larger than ideal for that particular ligand. The reflexive effect on the metal ion involves a compression or constriction that is applied to the metal ion leading to enhancement of Dq^{xy}. In contrast, [16]aneN$_4$ would fit best a metal having a larger M–N distance. Consequently, the larger cyclic ligand is compressed into an unfavorable M–N distance by the small Ni^{2+} ion. The excess strain energy in the ring, when bound this way, exerts an expanding or dilative effect on the NiN$_4$ coordination grouping with the result that Dq^{xy} is decreased. These relationships have been discussed in more detail in conjunction with the related cobalt(III) systems.[38]

Examination of Ni–N distances from x-ray structure determinations supports this view. Typical values of this distance fall around 2.13 Å for high spin Ni^{2+} [43] and the value for Ni(en)$_3^{2+}$ is 2.12 Å.[44] The average Ni–N distance in the folded, high spin, *cis*-[Ni([13]aneN$_4$)(NCS)$_2$] is also 2.12 Å indicating that a normal Ni–N distance can readily be achieved by folding.[41] In the low spin complex of Me$_3$[13]aneN$_4$, the Ni–N distance is quite short, 1.86 Å.[45] The great difference in these values supports the contention that the metal ion site in planar [13]aneN$_4$ is too small to accommodate high spin Ni^{2+}. Given that the normal Ni–N distance for high spin complexes is ~2.12 Å, the experimental value of 2.06 Å for Ni([14]aneN$_4$)Cl$_2$ is consistent with the high value of Dq^{xy} observed for that complex.[25]

Ring size effects are expected to appear in other chemical and physical properties of metal complexes. For nickel, the electrochemical studies reported earlier from these laboratories[35] show that the Ni^{2+}/Ni^{3+} couple shifts in favor of the trivalent state as the ring size decreases ($E_{1/2}$ = +1.3, +0.90, +0.69 v for Me$_6$[16]aneN$_4$, [15]aneN$_4$, and [14]aneN$_4$, respectively). Similarly, the Ni^{+}/Ni^{2+} progressively favors Ni^{+} over Ni^{2+} in the reverse direction ($E_{1/2}$ = −1.70, −1.57, −1.4 v for [14]aneN$_4$, [15]aneN$_4$, and Me$_6$[16]aneN$_4$, respectively). This is consistent with the expected changes in metal ion size with oxidation state.

The type and degree of unsaturation present in the macrocycles also has a profound effect on Dq^{xy} as is again apparent in Table IV. As the number of imine functions increases so does Dq^{xy} (from NCS$^-$ derivatives), e.g., Me$_2$[14]aneN$_4$ (1414 cm^{-1}), Me$_2$[14]1,3-dieneN$_4$ (1553 cm^{-1}), and Me$_4$[14]-1,3,8,10-tetraeneN$_4$ (1767 cm^{-1}). These increased values of Dq^{xy} are attributed essentially to two factors: (1) imines are stronger donors toward metal ions than are secondary amines; (2) the metal ion site in the rings is made smaller as the extent of unsaturation increases. This results in a shortened M–N distance and the net effect is the same as that discussed above for ring size. In essence, then, one can stay within the same chelated framework and ring size and still have control over the ligand field strength, increasing or decreasing it, depending on the extent of unsaturation. For example, Dq^{xy} for Ni([15]-aneN$_4$)(NCS)$_2$ is 1202 cm^{-1} and Dq^{xy} for Ni(Me$_6$[15]-4,12-dieneN$_4$)(NCS)$_2$ is 1232 cm^{-1}. The introduction of two isolated imine functions into the 16-membered has effectively increased the ligand field strength to that of the 15-membered ring. Several other examples showing the effect of adding double bonds on Dq^{xy} are

[14]aneN$_4$ → Me$_2$[14]1,3-dieneN$_4$, ΔDq^{xy} = 143 cm^{-1}
[14]aneN$_4$ → Me$_2$[14]4,11-dieneN$_4$, ΔDq^{xy} = 159 cm^{-1}
[16]aneN$_4$ → Me$_2$[16]4,12-dieneN$_4$, ΔDq^{xy} = 149 cm^{-1}

from these three examples we suggest that introducing two double bonds into the ring for $Ni(MAC)(NCS)_2$ increases Dq^{xy} by 150 cm^{-1} and that it does not matter whether the imine groups are conjugated or not. We add the caution that the latter conclusion requires Dq^{xy} to be insensitive to the extent of methyl substitution on the ligand.[46] The change in going from $Me_2[14]1,3\text{-dieneN}_4$ to $Me_4[14]1,3,8,10\text{-tetraeneN}_4$ is 214 cm^{-1} so that the addition of the second pair of double bonds has a greater effect on Dq^{xy} than does the addition of the first pair. It is reasonable to suggest that this enhanced response of Dq^{xy} is caused by more pronounced ring size effects that accompany the incorporation of four C=N distances into the macrocycle. It is interesting that the value of ΔDq^{xy} for putting four C=N groups in a 14-membered ring, as estimated from $[14]aneN_4 \rightarrow Me_6[14]1,3,8,10\text{-tetraeneN}_4$, whose value is 357 cm^{-1}, is very close to the value estimated for ΔDq^{xy} (= 350 cm^{-1}) for the 16-membered ring example $TAABH_8 \rightarrow TAAB$. In fact, the magnitude of this change is very similar to that associated with changing the ring size of a fully saturated ligand by two members; i.e., $[16]aneN_4 \rightarrow [14]aneN_4$, ΔDq^{xy} = 337 cm^{-1}.

In contrast to the results of electrochemical studies,[35] Dq^{xy} values are not sensitive to the presence of the sterically demanding axial methyl groups on the chelate rings. Comparing values for $[14]aneN_4$, $Me_2[14]aneN_4$, and $Me_6[14]aneN_4$, the average values are 1458, 1450, and 1443 cm^{-1}, respectively. The numbers are identical within experimental error. The small apparent trend is seen to be still less meaningful when attention is directed to the data for the bromide, the largest axial ligand. Here the small difference is actually of the opposite sign. The effect of axial methyl groups on Dq^z is, however, detectable as is pointed out below.

Having delineated the factors that contribute to the determination of Dq^{xy} in tetragonal complexes of the general formula $Ni(MAC)X_2$, it is of interest to examine the interrelationship between these structural parameters. This can be done by the simple device of examining the ΔDq^{xy} values for additivity. Using the results from the preceding discussion, the incremental values given in Table VII are assigned—$[15]aneN_4$ is chosen as the reference ligand because of its near ideal fit to high spin Ni^{2+} and the NCS axial ligand is chosen because it is associated with the largest series of complexes in Table IV.

The reproduction of the experimental data by the procedure implicit in Table VII is remarkable. The average difference between experimental and *recalculated* Dq^{xy} for 27 compounds is 0.7%; the greatest disagreement is 4%. The essentially complete additivity of these effects is shown in Figure 10, where the calculated and observed values are graphed and their positions compared to the slope = 1 line. The least-squares slope of the line is 1.01 and the correlation coefficient has a value of 0.994. The single point that is well off the line (4%) is that for $TAABH_8$ which contains unsaturation in its ring but only amine donors. The two ligands containing pyridine rings fused onto the chelating macrocycle have been omitted because they fail to correlate. In the case of $Me_2[14]py\text{-dieneN}_4$, the effect of the pyridine on Dq^{xy} is greater than that of two imine groups but in the case of $Me_2[14]py\text{-aneN}_4$, the Dq^{xy} value is the same as that of a fully saturated ligand. To incorporate these compounds in the correlation it would have been necessary to assume that py acts like a saturated group unless it is conjugated to an imine linkage, in which case it enhances Dq^{xy} as much as *two* imines.

The excellent agreement between calculated and observed values for the macrocyclic ligand derivatives indicates that the various structural parameters exert their effects with a measure of independence that is commensurate with the assumptions made in developing Table VII. It follows that one can expect to predict the Dq^{xy} values for a great many macrocyclic complexes with nickel(II) for which experimental values are not available.

Table VII. Contribution of Structural Changes[a] to Dq^{xy}

Structural change	ΔDq^{xy} (cm^{-1})
15-Membered ring → 14-membered ring	+210
15-Membered ring → 16-membered ring	−130
Amine → imine	+75
Special correction for change of 3rd and 4th amines to imines (per pair)	+80
NCS → N_3	+15
NCS → Cl	+50
NCS → Br	+70

[a] Reference compound is $Ni([15]aneN_4(NCS)_2$, Dq^{xy} = 1202 cm^{-1}.

Variation of Dq^z with Structure. Table IV is arranged to display the dependence of Dq^z on the nature of the in-plane ligand field. For each set of complexes $Ni(MAC)X_2$, where X is constant and MAC varies, Dq^z decreases as Dq^{xy} increases. This result is of considerable significance since the spectra of the more extensive sets of compounds previously reported as showing this effect earlier[10] were treated by inadequate methods and the phenomenon was necessarily in doubt. The limited data of Rowley and Drago[3] provided considerable support for this interpretation early on. Further, a related effect has been reported for copper(II).[47] Now it is certain that Dq^z is strongly influenced by the in-plane ligand field. This cis effect is shown graphically in Figure 11 where the thiocyanate complexes are chosen because their series is the most extensive. Regression analysis supports a linear correlation and the slope of the least-squares line is −0.33, the correlation coefficient is 0.82. Similar treatment gives slopes for the other axial ligands as follows: −0.54, Br; −0.54; Cl; and −0.39, N_3. (Correlation coefficients: 0.73, 0.72, and 0.71.) The slope, of course, reflects the sensitivity of the parameter Dq^z to changes in in-plane ligand field strength. It is noted that the weaker axial ligands are more sensitive to changes in the ligand field of the macrocycle. This sensitivity roughly approximates a linear dependence of the slope (see above) on Dq^z (on the basis of Dq^z values measured vs. $[15]aneN_4$). The sensitivity factor, ΣDq^z (the slope of the curve of Dq^z vs. Dq^{xy}), appears to obey the equation

$$\Sigma Dq^z = (5.12 \times 10^{-3})Dq^z - 0.797$$

for the very limited data treated.

The influence of Dq^z on the in-plane ligand field strength is an equally interesting manifestation of the *cis effect* in these complexes. Although only four axial ligands are available (Br, Cl, N_3, NCS—see Table IV), the linear correlation between Dq^{xy} and Dq^z for the constant in-plane ligands $[14]aneN_4$, $Me_6[14]aneN_4$, $[15]aneN_4$, and $[16]aneN_4$ is surprisingly good (Figure 12). The slopes and correlation coefficients are summarized below in Table VIII. The sensitivities, as reflected by the slopes of the lines in Figure 11, are similar for the four macrocycles and generally several times smaller than the sensitivities of the axial ligand Dq^z values to changes in the in-plane ligand field. To reiterate, Dq^{xy} varies in a linear fashion with changes in Dq^z but the changes are not so great as are the changes in Dq^z that occur when Dq^{xy} is varied.

Another factor that is apparent from these comparisons relates to the presence of axial CH_3 groups on the ligands. From the data in Table IV, the presence of these substituents causes a decrease in Dq^z by a substantial amount. In terms of percentage change, the effect is greatest with the large bromide axial ligand.

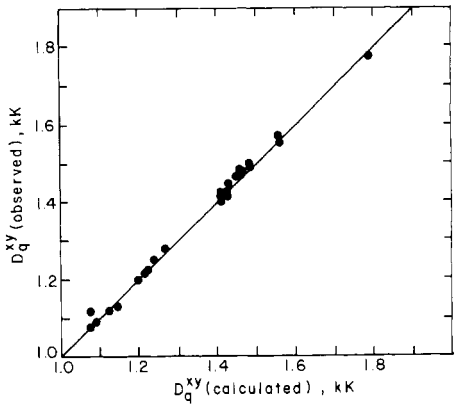

Figure 10. Additivity of structual contributions to Dq^{xy} for Ni^{2+} complexes with macrocyclic ligands. 1 μm^{-1} = 10 kK.

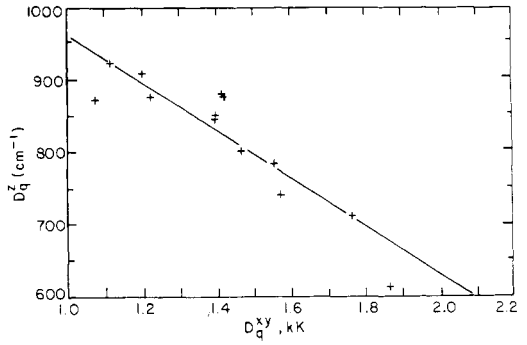

Figure 11. Changes in Dq^z for NCS as Dq^{xy} are varied among the complexes Ni(MAC)$(NCS)_2$. 1 μm^{-1} = 10 kK.

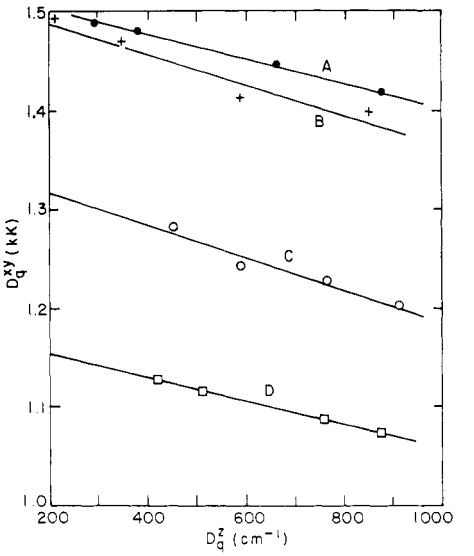

Figure 12. Changes in Dq^{xy} for a given macrocycle as Dq^z vary among the complexes Ni(MAC)X_2 (X = Br, Cl, N_3, NCS): A, MAC = [14]-aneN$_4$; B, MAC = Me_6[14]aneN$_4$; C, MAC = [15]aneN$_4$; D, MAC = [16]aneN$_4$. 1 μm^{-1} = 10 kK.

Table VIII

Ligand	Slope	Correlation coefficient
[14]aneN$_4$	−0.119	0.997
Me_6[14]aneN$_4$	−0.152	0.932
[15]aneN$_4$	−0.166	0.946
[16]aneN$_4$	−0.118	1.000

Variations of Other Parameters with Structure. The working parameters in the weak field model are *Dt*, *Ds*, and *B*. The former, *Dt*, represents the tetragonal splitting parameter which is related to the fourth degree spherical harmonics of the perturbing ligand field while *Ds* is the second degree tetragonal splitting parameter. From the defining equation

$$Dq^z = Dq^{xy} - 1.75Dt$$

Dt forms the basis for the calculation of Dq^z and the behaviors of the two parameters are of necessity strictly parallel. The parameter *Ds* is associated with the splittings of the second and third bands ($^3T_{1g}$(P) and $^3T_{1g}$(F) in O_h). While not highly systematic, the variations in *Ds* generally follow the same pattern as *Dt*.

The parameters of the strong field model might be expected to be more meaningful in interpreting the chemical properties of these substances. Indeed, Dq^{xy} is Δ_2 of the strong field model. Dq^z cannot be identified with a single orbital splitting in the strong field case—eq 7 defines Dq^z.

$$Dq^z = Dq^{xy} + (1/20)(4\Delta_1 - 3\Delta_3)$$
$$= \Delta_2 + (1/5)\Delta_1 - (3/20)\Delta_3 \quad (7)$$

However, Table IV shows that so long as $Dt > 200$, the value of Δ_3 exceeds that of Δ_1 by a factor of seven or more. Under these conditions, Dq^z is related to Δ_3 in essentially the same way it is related to *Dt*

$$Dq^z = Dq^{xy} - 1.75Dt$$
$$Dq^z \cong Dq^{xy} - (3/20)\Delta_3$$

The results show Δ_1 to be small and variable in both magnitude and sign. This is not unexpected since Δ_1 represents the splitting in the t_{2g} orbitals. In view of the small size of this parameter we have not attempted to interpret its variations here. In contrast, Δ_3, the splitting between the d_{z^2} and $d_{x^2-y^2}$ orbitals of the eg set, is generally quite large and correlates well with the difference between the axial and in-plane ligand fields.

The interelectronic repulsion parameter *B* is expected to exhibit values in the range from 800 to 900 cm^{-1} in complexes of high spin Ni^{2+} with ligands of the sort reported here.[3,48] The values for this parameter listed in Table IV appear to move randomly from structure to structure. This is partly due to the fact that exact band assignments for $^3E_g{}^c$ and $^3A_{2g}{}^b$ are required in order to derive a precise value for *B*.

Experimental Section

Physical Measurements. The infrared spectra were obtained on a Perkin-Elmer Model 337 recording spectrometer using Nujol mulls mounted between KBr disks. Polystyrene standards were used to calibrate spectra. Conductivity measurements were performed with an Industrial Instruments Model RC 16B conductivity bridge at 25 °C at 1000 Hz on 10^{-3} M solutions. Mass spectral measurements were carried out on an MS-9 spectrometer, at an ionizing potential of 70 eV, using a direct insertion probe. Proton magnetic resonance spectra (^{1}H NMR) were obtained on a JEOL-100 spectrometer.

Magnetic measurements on solid samples were performed at room temperature under 33 mm of helium gas using the Faraday method.[49]

Electronic absorption spectra were obtained with a Model 14R Cary spectrophotometer equipped with a high intensity light source. Solution spectra were obtained in 1- or 5-cm quartz cells. Solid state spectra, both at room temperature and liquid nitrogen temperature, were taken as mulls on filter paper. Halocarbon-25-5S grease was employed as the mulling agent. The compounds were ground in the mulling agent until a fine particle size was obtained. The mulls were then applied to filter paper strips and placed in an appropriate Dewar. The concentration of the mulls was such that an absorbance of 0.6–0.7 was observed. Direct immersion into liquid nitrogen was used to obtain spectra.

The Ohio State University Instructional and Research Computer

Center IBM 7094, IBMs/360/75, IBM 1629, IBM 1130 computing systems were used to perform all calculations. All programs used were either written or modified by Sperati.[6]

Syntheses. All materials were reagent grade and used without further purification.

[13, 14, 15, and 16]aneN$_4$. Ligand structures are shown in Figure 1. The procedure follows Scheme I. The individual steps are described below.

Tosylated Linear Tetramines. *N,N',N'',N'''*-Tetra-*p*-toluenesulfonyl derivatives of triethylenetetramine (2.2.2), *N,N'*-bis(2-aminoethyl)-1,3-diaminopropane (2.3.2), *N,N'*-bis(3-aminopropyl)-1,2-diaminoethane (3.2.3), and *N,N'*-bis(3-aminopropyl)-1,3-diaminopropane (3.3.3) were starting materials for the [13, 14, 15, and 16]aneN$_4$ macrocyclic rings, respectively. To a solution of the appropriate linear tetramine (0.1 mol) and sodium hydroxide (0.4 mol) in water (108 mL), there is added dropwise, a solution of *p*-toluenesulfonyl chloride (0.4 mol) in ether (400 mL). The mixture is then stirred for 1 h at room temperature. The tosylates are solids except for the 2.3.2 derivative which remains a viscous oil. The solids are recrystallized from large volumes of methanol (1–2 L) while the 2.3.2 tosylate is used in succeeding steps without further purification.

***N,N',N'',N'''*-Tetra(*p*-toluenesulfonyl) Derivatives of [13, 14, 15, and 16]aneN$_4$.** To a vigorously stirred mixture of anhydrous potassium carbonate (20 g) in dimethylformamide (1 L) at 120 °C, there is added, at a rate of 1 drop per 10 s, a solution of the tosylated tetramine (0.015 mol) and 1,3-dibromopropane (0.015 mol) in dimethylformamide (267 mL). The total time for addition is about 20 h. The mixture is stirred for an additional 7 h at 115–120 °C after the addition is completed. Upon cooling to room temperature the solution is filtered to remove any inorganic precipitates. The filtrate is rotoevaporated to approximately 100 mL.[50] Water (1.5 L) is then added to deposit a tacky, off-white precipitate which is extracted with hot benzene (1 L). The benzene extract is dried for approximately 5 h over anhydrous sodium sulfate. The benzene is rotoevaporated to about 150 mL. The addition of alcohol (100–200 mL) followed by refrigeration for several hours results in the precipitation of a white powder, which is washed with two–three (10 mL) portions of alcohol.

Hydrolysis of Tosyl Groups. The tosylated [13–16]aneN$_4$ (0.004 mol) is dissolved by heating it in 30% hydrobromic–acetic acid (300 mL), which is prepared by adding nine volumes of glacial acetic acid to 16 volumes of 47% hydrobromic acid. Refluxing is continued until dissolution occurs (1–2 days).[51] The volume of the solution is reduced to one-tenth its initial volume; after cooling, ether (200 mL) is added to separate a solid which is washed repeatedly with ether and then alcohol. The product is air dried on the frit.

Free Ligand Extraction. The tetrahydrobromide salt of [13–16]-aneN$_4$ is dissolved in a minimum amount of water and is neutralized with a slight excess over the stoichiometric amount of sodium hydroxide. Several extractions with chloroform are then carried out. The chloroform is flash evaporated, ether is added and then flashed off leaving behind the solid ligand. Sometimes, especially in the case of [13]aneN$_4$, refrigeration is required to bring about solidification of the ligand. These ligand syntheses readily avail themselves to scale up.

[Ni([15]aneN$_4$)](ClO$_4$)$_2$. A methanolic solution containing 0.5 g (0.0023 mol) of ligand and 0.84 g (0.0023 mol) of nickel(II) perchlorate 6-hydrate is warmed for ≈15 min. The solution is a dirty orange color. It is filtered and the volume is reduced on the rotary evaporator. An orange, crystalline product is isolated. Yield ≈75%.

[Ni([15]aneN$_4$)Cl$_2$] and [Ni([15]aneN$_4$)Br$_2$]. These complexes are prepared by dissolving 0.5 g (0.0023 mol) of ligand in 50 mL of methanol and adding 0.58 g (0.0023 mol) of nickel(II) acetate 4-hydrate. The blue-violet solution is warmed gently for approximately 15 min. A slight excess of the appropriate lithium salt is added and the solution lightens somewhat in color. The solution is warmed for an additional 5–10 min. Rotoevaporation of the methanol to dryness results in a purple solid. The solid is dissolved in chloroform and filtered to remove any unreacted nickel salt, after which the chloroform is flashed off. This procedure is repeated twice. The products are recrystallized from acetonitrile and dried in vacuo for several hours. Yield ≈50%.

[Ni([15]aneN$_4$)(N$_3$)$_2$]. The same procedure is employed here as for the bromide and chloride derivatives, except that the reaction is conducted in alcohol. Again, the appropriate lithium or sodium salt is used. Acetonitrile is employed to recrystallize the complex. Yield ≈45%.

[Ni([15]aneN$_4$)(NCS)$_2$]. Again the same procedure is applied for this complex, the difference being in the solvent used to carry out the reaction. This reaction is conducted in water. The blue solution of the ligand nickel salt becomes lavender when lithium or sodium thiocyanate is added. The product has a limited solubility in water and as a result readily precipitates from the water solution during the course of the reaction. The product is recrystallized from hot water. The yield is virtually quantitative.

[Ni([16]aneN$_4$)](ClO$_4$)$_2$, [Ni([16]aneN$_4$)Cl$_2$], [Ni([16]aneN$_4$)Br$_2$], [Ni([16]aneN$_4$)(N$_3$)$_2$], and [Ni([16]aneN$_4$)(NCS)$_2$]. This series of complexes is prepared in an identical fashion with the 15-membered ring derivatives. The orange perchlorate derivative and the blue thiocyanate derivative are recrystallized from methanol. The pale green chloride and bromide derivatives and the blue-green azide derivative are recrystallized from acetonitrile. These derivatives are dried in vacuo for several hours. The yields or these complexes are similar to those observed for the 15-membered ring derivatives.

Ni([14]aneN$_4$)(N$_3$)$_2$. Ni([14]aneN$_4$)(ClO$_4$)$_2$ (1 mmol) was dissolved in 30 mL of ethanol and a saturated ethanol solution of potassium thiocyanate was added. After heating for 10 min on a steam bath, the solution was filtered to remove the potassium perchlorate. The solution was then evaporated to dryness. The resulting mauve solid was extracted into chloroform and reprecipitated by the addition of ether to the cloud point followed by cooling. Yield 55%.

Ni(Me$_2$[14]1,3-dieneN$_4$)X$_2$ and Ni(Me$_4$[14]1,3,8,10-tetraeneN$_4$)X$_2$ Complexes. These high spin thiocyanate derivatives were prepared from (2,3-dimethyl-1,4,8,11-tetraazacyclotetradeca-1,3-diene)-nickel(II) perchlorate and (2,3,9,10-tetramethyl-1,3,8,10-tetraazacyclotetradeca-1,3,8,10-tetraene)nickel(II) perchlorate by metathetical reaction.

Ni(Me$_2$[14]1,3-dieneN$_4$)(ClO$_4$)$_2$. Twenty millimoles of (3.2.3) was dissolved in 150 mL of dry methanol and 20 mmol of concentrated HCl was added. Twenty millimoles of biacetyl was added to this solution. The resulting yellow solution was allowed to stand at room temperature without stirring for 30 min, during which time the color changed. At this point 20 mmol of nickel acetate 4-hydrate was added and the solution was stirred at room temperature for 4 h. After this time, a saturated 50-mL methanol solution of $ZnCl_2$ was filtered into the reaction mixture and stirring was continued for 1 h. The red-brown precipitate that formed was collected by filtration. An aqueous solution of the tetrachlorozincate salt was treated with $AgNO_3$ and filtered, followed by $NaClO_4$. Concentrating the solution produced a yellow crystalline material which was recrystallized from methanol by the addition of ether.

Ni(Me$_4$[14]1,3,8,10-tetraeneN$_4$)(ClO$_4$)$_2$. A procedure analogous to that stated above utilizing 1,3-diaminopropane monohydrochloride (prepared in situ with concentrated HCl) in place of the 3.2.3 was employed to prepare this complex.

Ni(Me$_2$[14]1,3-dieneN$_4$)(NCS)$_2$. Ten millimoles of Ni(Me$_2$-[14]1,3-dieneN$_4$)(ClO$_4$)$_2$ was dissolved in 75 mL of absolute ethanol and a 2 mL saturated aqueous solution of potassium thiocyanate was added. The solution was heated on a steam bath for half an hour. After filtering to remove insoluble potassium perchlorate the filtrate was evaporated to dryness. Extraction into chloroform followed by the addition of ether to induce crystallization produced a dark purple-brown solid. The product was washed with ether, then dried over P_4O_{10} in vacuo. The compound is slightly moisture sensitive. Yield 45%.

Ni(Me$_4$[14]1,3,8,10-tetraeneN$_4$)(NCS)$_2$. Ten millimoles of Ni(Me$_4$[14]1,3,8,10-tetraeneN$_4$)(ClO$_4$)$_2$ was dissolved in 75 mL of absolute ethanol and a 2-mL saturated aqueous solution of potassium thiocyanate was added. The solution was heated on a steam bath for half an hour after which the insoluble potassium perchlorate was removed by filtration. The red-purple filtrate was evaporated to dryness and the resulting solid was dissolved in chloroform. Crystallization was initiated with ether. The red-brown solid was washed with ether and dried over P_4O_{10} in vacuo. The sample was slightly moisture sensitive.

Ni(Me$_2$[14]aneN$_4$)X$_2$ Complexes. The chloride, bromide, azide, and thiocyanate complexes were prepared either from the free ligand and the appropriate metal salt or by metathesis from the perchlorate salt.

Ni(Me$_2$[14]aneN$_4$)(ClO$_4$)$_2$. Twenty grams of Ni(Me$_2$[14]1,3-dieneN$_4$)(ClO$_4$)$_2$ is dissolved in 400 mL of water to produce a dark orange solution. It is then poured into a pressure bottle with 5 g of active Raney nickel catalyst No. 28 and placed on a hydrogenation apparatus under 50 lb of pressure. After 24 h, hydrogen uptake is

complete.

The catalyst is removed by filtration and the methanol is evaporated under reduced pressure. The catalyst is very pyrophoric at this point and must be kept wet. It is decomposed by reaction with dilute HCl. The yellow-orange solid is recrystallized from methanol and dried in vacuo.

Isolation of the Free Ligand 2,3-Dimethyl-1,4,8,11-tetraazacyclotetradecane, $Me_2[14]aneN_4$. $Ni(Me_2[14]aneN_4)(ClO_4)$ (4.1 mmol) is refluxed in 150 mL of water containing 3 g of NaCN for 1.5 h. The solution is cooled and extracted five times with 20 mL of $CHCl_3$. The extracts are dried over sodium sulfate and evaporated to dryness under reduced pressure. The resulting white solid is recrystallized from THF to give 0.8 g of white needles. Yield 75%.

$Ni(Me_2[14]aneN_4)Cl_2$. Twenty millimoles of nickel(II) chloride 6-hydrate is dissolved in 50 mL of absolute ethanol. To this is added 15 mL of triethylorthoformate and the solution is refluxed for 45 min. A 10-mL solution containing 18 mmol of ligand is added to this hot solution. After heating for 15 min, followed by concentrating and cooling, a mauve precipitate forms. The precipitate is recrystallized from chloroform with the addition of ether to induce crystallization.

An alternative method of preparation involves dissolution of 20 mmol of $Ni(Me_2[14]aneN_4)(ClO_4)_2$ in 50 mL of hot absolute ethanol and addition of a 1-mL saturated aqueous solution of potassium chloride. After heating for 15 min on a steam bath, the purple solution is filtered to remove the insoluble potassium perchlorate. It is then evaporated to dryness under reduced pressure. Recrystallization of the moisture-sensitive product from a chloroform–ether mixture produces mauve crystals which are collected in a glove box, washed with ether, and dried in vacuo.

$Ni(Me_2[14]aneN_4)Br_2$. The procedure for the preparation of this compound is identical with that for the chloride complex, using, however, either nickel(II) bromide 6-hydrate or potassium bromide as starting material depending on which preparative technique is used. $Ni(Me_2[14]aneN_4)Br_2$ has a greater moisture sensitivity than the chloride complex.

$Ni(Me_2[14]aneN_4)(N_3)_2$ and $Ni(Me_2[14]aneN_4)(NCS)_2$. Both complexes are prepared by metathesis from the corresponding perchlorate derivative. To a 20-mmol ethanol solution of $Ni(Me_2[14]aneN_4)(ClO_4)_2$ is added a 2-mL saturated aqueous solution of the appropriate potassium salt. The solution is heated on a steam bath for 20 min. After filtration to remove precipitated potassium perchlorate, the purple solution is evaporated to dryness under reduced pressure. The mauve solid is recrystallized from chloroform to remove extraneous salts.

Acknowledgment. The support of this research by a grant from the National Science Foundation is greatly appreciated.

References and Notes

(1) The abbreviations used follow the system previously described (V. L. Goedken, P. H. Merrell, and D. H. Busch, *J. Am. Chem. Soc.*, **94,** 3397 (1972)).
(2) C. J. Ballhausen, "Introduction to Ligand Field Theory", McGraw-Hill, New York, N.Y., 1962.
(3) D. A. Rowley and R. S. Drago, *Inorg. Chem.*, **6,** 1092 (1967); **7,** 795 (1968).
(4) A. B. P. Lever, *Coord. Chem. Rev.*, **3,** 119 (1968).
(5) A. B. P. Lever, *Adv. Chem. Ser.*, **No. 62,** 430 (1967).
(6) C. R. Sperati, Ph.D. Thesis, The Ohio State University, 1971.
(7) O. G. Holmes and D. S. McClure, *J. Chem. Phys.*, **26,** 1686 (1957).
(8) R. A. D. Wentworth and T. S. Piper, *Inorg. Chem.*, **4,** 709, 1524 (1965).
(9) G. R. Brubaker and D. H. Busch, *Inorg. Chem.*, **5,** 2114 (1966).
(10) D. H. Busch, *Helv. Chim. Acta, Werner Commemoration Volume,* 174 (1967).
(11) A. B. P. Lever, "Inorganic Electronic Spectroscopy", Elsevier, Amsterdam, 1968.
(12) F. R. Fenske, D. S. Martin, Jr., and K. Reudenberg, *Inorg. Chem.*, **1,** 441 (1962).
(13) N. F. Curtis and R. W. Hay, *Chem. Commun.*, 524 (1966).
(14) A. M. Tait and D. H. Busch, *Inorg. Nucl. Chem. Lett.*, **8,** 491 (1972).
(15) E. K. Barefield, *Inorg. Chem.*, **11,** 2273 (1972).
(16) E. S. Gore, E. K. Barefield, and D. H. Busch, unpublished results.
(17) D. A. Baldwin and N. J. Rose, Abstracts of the 157th Meeting of the American Chemical Society, Minneapolis, Minn., 1967.
(18) G. A. Melson and D. H. Busch, *J. Am. Chem. Soc.*, **86,** 4830 (1964).
(19) E. K. Barefield, F. V. Lovecchio, N. E. Tokel, E. Ochiai, and D. H. Busch, *Inorg. Chem.*, **11,** 283 (1972).
(20) J. van Alphen, *Recl. Trav. Chim. Pays-Bas,* **56,** 343 (1937).
(21) H. Stetter and K. H. Mayer, *Chem. Ber.*, **94,** 1410 (1961).
(22) H. Koyama and T. Yoshino, *Bull. Chem. Soc. Jpn.*, **45,** 481 (1972).
(23) B. Bosnich, C. K. Poon, and M. L. Tobe, *Inorg. Chem.*, **4,** 1109 (1965).
(24) The first data at longer wavelengths were obtained by E. K. Barefield, Ph.D. Thesis, The Ohio State University, 1969.
(25) B. Bosnich, R. Mason, P. T. Pauling, G. B. Robertson, and M. L. Tobe, *Chem. Commun.*, 97 (1965).
(26) J. C. Donini, B. R. Hollebone, and A. B. P. Lever, *J. Am. Chem. Soc.*, **93,** 6455 (1971).
(27) We thank Dr. Virgil Goedken for assistance in mounting and aligning the crystal.
(28) F. A. Cotton, "Chemical Applications of Group Theory", 2nd ed, Wiley-Interscience, New York, N.Y., 1971.
(29) P. Krumholz, *Struct. Bonding (Berlin),* **9,** 139 (1970).
(30) K. M. Long and D. H. Busch, *J. Coord. Chem.*, **4,** 113 (1974).
(31) S. C. Jackels, K. Farmery, E. K. Barefield, N. J. Rose, and D. H. Busch, *Inorg. Chem.*, **11,** 2893 (1972).
(32) See for example: F. A. Cotton and G. Wilkinson, "Advanced Inorganic Chemistry", 3rd ed, Interscience, New York, N.Y., 1972, p 604.
(33) M. C. Rakowski and D. H. Busch, *J. Am. Chem. Soc.*, **97,** 2570 (1975).
(34) J. C. Dabrowiak and D. H. Busch, *Inorg. Chem.*, **14,** 1881 (1975).
(35) F. V. Lovecchio, E. S. Gore, and D. H. Busch, *J. Am. Chem. Soc.*, **96,** 3109 (1974).
(36) F. Basolo and R. G. Pearson, *Prog. Inorg. Chem.*, **4,** 447 (1962).
(37) L. Y. Martin, L. J. DeHayes, L. J. Zompa, and D. H. Busch, *J. Am. Chem. Soc.*, **96,** 4046 (1974).
(38) Y. Hung, L. Y. Martin, S. Jackels, and D. H. Busch, submitted for publication.
(39) C. G. Spike and R. W. Parry, *J. Am. Chem. Soc.*, **75,** 2726 (1953).
(40) L. Y. Martin, Ph.D. Thesis, The Ohio State University, 1974.
(41) P. W. R. Corfield and S. Yang, unpublished results.
(42) We choose to emphasize the values reported in ref 6 because they are based on low temperature measurements and the same detailed spectral analysis reported here.
(43) P. O. Whimp, M. F. Bailey, and N. F. Curtis, *J. Chem. Soc. A,* 1956 (1970).
(44) L. N. Swink and M. Atoji, *Acta Crystallogr.*, **13,** 639 (1960).
(45) J. M. Waters and K. R. Whittle, *J. Inorg. Nucl. Chem.*, **34,** 155 (1972).
(46) Axial CH_3 groups have been shown to effect $E_{1/2}$ for the Ni^{2+}/Ni^{3+} couple (ref 35).
(47) A. B. P. Lever and E. Mantovani, *Inorg. Chem.*, **10,** 817 (1971).
(48) C. K. Jorgensen, *Prog. Inorg. Chem.*, **4,** 73 (1962).
(49) L. L. Lindoy, V. Katović, and D. H. Busch, *J. Chem. Educ.*, **49,** 117 (1972).
(50) Exceptions to regular reaction workup were applied to the $[16]aneN_4$ system. The tosylated $[16]aneN_4$ has a tendency to incorporate DMF. As a result, its solubility is decreased and it precipitates as the DMF solvate when rotoevaporated. The solid is filtered, washed with DMF, and then water. The filtrate is then treated according to the stated procedures. It should be noted that the major portion of the product precipitates as the tosylated $[16]aneN_4 \cdot x$DMF adduct, consequently only a small amount is obtained following normal workup procedures.
(51) For the $[16]aneN_4$ solubility is once again a problem. Dissolution is never observed because of the low solubility of the $[16]aneN_4 \cdot 4HBr$ in the acid system. To ensure complete hydrolysis, the mixture is refluxed for 4 days. At this time, there is a noticeable change in the color and consistency of the heterogeneous system. The mixture is red-brown in color and the solid has an iridescent quality to it. The mixture is filtered through *filter aid.* The filtrate is treated as previously described to yield additional $[16]aneN_4 \cdot 4HBr$. The product on the filter aid is then washed with warm water until all of it has dissolved. The water is rotoevaporated to approximately 100 mL. Ethanol and ether are added to precipitate the $[16]aneN_4 \cdot 4HBr$. This workup accounts for approximately 90% of the ligand salt.